RSC Advances

REVIEW

View Article Online
View Journal | View Issue

Cite this: *RSC Adv.*, 2023, **13**, 19540

New insights into nanosystems for non-small-cell lung cancer: diagnosis and treatment

Piao Jiang,†[ab] Bin Liang,†[a] Zhen Zhang,†[c] Bing Fan,[d] Lin Zeng,[a] Zhiyong Zhou,[a] Zhifang Mao,[a] Quan Xu,*[e] Weirong Yao*[a] and Qinglin Shen *[ac]

Received 9th May 2023
Accepted 12th June 2023

DOI: 10.1039/d3ra03099g

rsc.li/rsc-advances

Lung cancer is caused by a malignant tumor that shows the fastest growth in both incidence and mortality and is also the greatest threat to human health and life. At present, both in terms of incidence and mortality, lung cancer is the first in male malignant tumors, and the second in female malignant tumors. In the past two decades, research and development of antitumor drugs worldwide have been booming, and a large number of innovative drugs have entered clinical trials and practice. In the era of precision medicine, the concept and strategy of cancer from diagnosis to treatment are experiencing unprecedented changes. The ability of tumor diagnosis and treatment has rapidly improved, the discovery rate and cure rate of early tumors have greatly improved, and the overall survival of patients has benefited significantly, with a tendency to transform to a chronic disease with tumor. The emergence of nanotechnology brings new horizons for tumor diagnosis and treatment. Nanomaterials with good biocompatibility have played an important role in tumor imaging, diagnosis, drug delivery, controlled drug release, *etc.* This article mainly reviews the advancements in lipid-based nanosystems, polymer-based nanosystems, and inorganic nanosystems in the diagnosis and treatment of non-small-cell lung cancer (NSCLC).

1. Introduction

Lung cancer, a major cause of cancer-related mortality worldwide, can be categorized into small cell lung cancer (SCLC) and non-small-cell lung cancer (NSCLC), with the latter accounting for approximately 80–85% of all cases.[1,2] Traditionally, NSCLC is diagnosed based on patients' medical history, signs, and symptoms, using imaging techniques such as X-ray, CT, MRI, fine needle aspiration biopsy of lung tissue, and thoracocentesis.[3,4] However, patients developing NSCLC are often detected as late as at stage III or IV, attributed to the absence of clinical symptoms in incipient stages, thus setting requirements for the early diagnosis of NSCLC.

The treatments of NSCLC are primarily composed of chemotherapy, radiotherapy, surgery, and emerging technologies such as targeted therapy, immunotherapy, photothermal therapy, and photodynamic therapy (PDT).[5–7] Despite some progress in the treatment of NSCLC, the five-year survival rate has only increased by 5% in recent years partially due to the lack of tumor targeting.[8] Accordingly, novel therapy with increased anti-tumor effect and reduced systemic cytotoxicity against NSCLC is urgently demanded.

Notably, natural or acquired resistance is one of the major challenges related to NSCLC treatment. Generally, resistance to chemotherapy is categorized into three types: kinetic, biochemical, and pharmacologic. Cell kinetics-related resistance is a special problem with many tumors because certain cells are in a plateau growth phase with a small growth fraction. Methods to overcome cell kinetics-related resistance involve: diminishing the volume of the tumors *via* surgery or radiotherapy; impacting G0 cells *via* combination drugs; and scheduling drugs to avoid phase escape or to synchronize cell groups and enhance cancer cell removal. The mechanism of biochemical resistance is not fully understood. Cancer cells undergoing this kind of resistance may show declined drug uptake, enhanced efflux, altered levels or structure of the intracellular target, downregulated intracellular activation, augmented drug inactivation, or accelerated repair of damaged DNA. Another example is multidrug resistance (MDR), a complex phenotype whose predominant feature is resistance to a wide range of structurally unrelated cytotoxic compounds. MDR is associated with a variety of mechanisms, including enhanced efflux of drugs, genetic factors (gene mutations, amplifications, and epigenetic alterations), growth factors, increased DNA repair capacity, and elevated metabolism of

[a]*Department of Oncology, Jiangxi Provincial People's Hospital, The First Affiliated Hospital of Nanchang Medical College, No. 152 Aiguo Road, Donghu District, Nanchang 330006, China. E-mail: qinglinshen@whu.edu.cn*

[b]*The First Clinical Medical College, Nanchang University, Nanchang, China*

[c]*Institute of Clinical Medicine, Jiangxi Provincial People's Hospital, The First Affiliated Hospital of Nanchang Medical College, Nanchang, China*

[d]*Department of Radiology, Jiangxi Provincial People's Hospital, The First Affiliated Hospital of Nanchang Medical College, Nanchang, China*

[e]*Department of Thoracic Surgery, Jiangxi Provincial People's Hospital, The First Affiliated Hospital of Nanchang Medical College, Nanchang, China*

† These authors contributed equally to this work.

xenobiotics. As for pharmaceutical resistance, it can be caused by poor tumor blood supply, poor or erratic absorption, enhanced excretion or catabolism, and drug interactions, all of which result in insufficient drug content in the blood.[9,10]

To overcome these limitations, it is paramount to develop innovative diagnosis and treatment technology targeted NSCLC. Nanomedicine, emerging as a propitious paradigm in cancer detection and therapy, has attracted more and more attention in the field of anti-NSCLC, because nanosystems offer flexible and fast drug design and production on the basis of tumor genetic profiles, leading to much more rational and effective drug selection for personalized patient treatment. The diagnosis or therapeutic efficacy of nanosystems can be manipulated by regulating their structure, geometry, materials, and surface chemistry.[11–13] Aside from utilizing biosensor devices-based nanoparticle-like gold nanorods that possess the property of imaging triggered by near-infrared light (NIR) irradiation,[14–16] another approach for theranostic nanomedicine is to conjugate or encapsulate both therapeutic and imaging agents to the designed nanoparticles.

Given the critical role of nanomedicine in the theranostics of NSCLC, this article aims to review the recent advance and progress of nanosystems in the early detection and improved anti-tumor effect against NSCLC. This review elucidates a wide variety of nanosystems including lipid-based nanoparticles, polymer-based nanoparticles, and inorganic nanosystems. We focus on the application of these nanosystems in the diagnosis and therapy of NSCLC and summarize recent advances in all kinds of nanosystems, which are illustrated by examples. Finally, we provide our perspective on the challenges and potential opportunities of nanosystems applied in the theranostics of NSCLC in the future.

2. Common characteristics of nanosystems

2.1. Advantages of nanosystems

2.1.1 Nanosize. Nanosystems with a diameter less than 5 nm are rapidly cleared from the circulation *via* extravasation or renal clearance, while those with a diameter ranging from ~10 nm to ~15 μm show diverse biodistribution, of which cellular uptake of nanosystems in this range is immensely up to the cell type. Normally, nanosystems are trapped by the filtration of the sinusoids in the spleen, followed by their removal from circulation through cells of the reticulo-endothelial system (RES).[17–19] Spherical nanosystems with a diameter of 100–200 nm have the highest potential for prolonged circulation considering that they are large enough to avoid uptake in the liver, while small enough to avoid filtration in the spleen. For long-circulating nanosystems, uptake by the liver and the spleen should be avoided, which can be nearly achieved *via* engineering deformability into sizes >300 nm or by keeping at least one dimension of the nanosystem on a length scale >100 nm to avoid accumulation in the liver, and meanwhile, maintaining at least two dimensions at <200 nm, thus allowing the nanosystem to pass the sinusoids of the spleen.[20]

2.1.2 Surface chemistry. These characteristics of nanosystems mainly exert two critical roles. First, it can greatly affect the process of opsonization, which finally dictates the RES response. On the other hand, it can realize cellular or organelle targeting through the attachment of ligands to the surface of the engineered nanosystems.[20,21] The ligands are known to bind to receptors that are overexpressed on the surface of rapidly dividing cancer cells. Active targeting strategies of nanosystems against NSCLC are summarized in Tables 2 and 3.

2.1.3 Stimuli-responsive release of cargo. Nanomaterials that respond either to an internal stimulus such as pH or to an external stimulus such as light, magnetic field, and ultrasound can be synthesized. These stimuli are applied as triggers to break covalent bonds between the carrier and cargo, or to destabilize the carrier, hence promoting the release of its contents once the carrier has reached a specific site.

The pH in the tumor tissues (pH of 5.4) and late endosomes and lysosomes (pH of 4.5–5.5) is lower than that in the healthy tissues and blood circulation (pH of 7.4). The acidic microenvironment in the tumor may lead to partial protonation of the amino, carboxylate, and phosphate groups of the nanosystems, and/or the cleavage of certain chemical bonds, which are unstable under acidic conditions such as hydrazide bonds. This impairs the interaction between nanosystems and guest molecules, thereby resulting in the selective release of cargo into tumors.[22]

Light-triggered theranostics has gained increasing attention owing to its high spatiotemporal precision, real-time dose control, wide clinical application in tumor imaging, photosensitizers (PSs)-based cancer killing through local hyperthermia, ROS or $^1O_2$, and the option for on-demand switching on and off modes. However, the major issue of limited tissue penetration heavily restricts the application against tumors located deep in the tissues. The NIR region (650 to 900 nm) is considered the 'biological window' because most of the body components such as blood and soft tissues do not absorb or scatter light in this wavelength region, providing access to non-invasive and deep tissue penetration for imaging and therapeutic goals. Heat and $^1O_2$ production are the most crucial effectors in light-triggered treatment. Hyperthermia (HT) caused by PS-induced heat generation leads to cell death, which is referred to as photothermal therapy (PTT). Increasing the temperature of the tumor microenvironment to 42 °C can cause cell damage and make cancer cells vulnerable to combined treatments such as irradiation and chemotherapy. When the temperature increases to 45 °C or above, it can have immediate lethal effects on the cells. On the other hand, $^1O_2$ is responsible for causing irreversible damage to intracellular organelles, also known as photodynamic therapy (PDT). Notably, the extremely short lifespan (<3.5 μs) and highly restricted diffusion (~10 to 20 nm) of $^1O_2$ can be used for localized apoptosis, necrosis, or autophagy-induced cell death.[23–25] Besides, light-based imaging techniques such as fluorescence, photoacoustic (PA) signal, and surface-enhanced Raman scattering (SERS) are useful in live bioimaging, namely optical imaging.[26]

Magnetic field (MF) is a widely applied physical trigger of magnetic nanosystems that can produce heat under an

oscillating MF, or be magnetically directed to lesion sites. Also, MF is widely utilized for magnetic resonance imaging (MRI) of tumor tissue. Unlike optical imaging, MF at frequencies below 400 Hz, is not readily absorbed by tissues, allowing remote monitoring without physical contact.[27]

Ultrasound (US) is another non-invasive stimulus utilized to trigger site-specific drug release and allows for spatiotemporal control with millimeter precision. A focused US beam can lead to drug release through localized heating produced by the accumulation of acoustic energy at the focused region.[28] The US imaging contrast agents (UCAs) are widely used in clinical examinations in order to improve the image resolution of the US. UCAs are acoustically active to external US energy, thus amplifying echo signals and improving image resolution based on differential echogenicity. The larger acoustic impedance difference between the solid phase and soft tissues indicates that compared with softer UCAs, inorganic NPs with rigid structures can yield better US image resolution.[29]

2.1.4 Biomimetic nanomaterials. The cell membrane-camouflaged nanosystems are a class of biomimetic nanosystems, which combine the unique functionalities of cellular membranes and the engineering versatility of synthetic nanomaterials for the effective delivery of therapeutic or imaging agents. Cell membrane-camouflaged nanosystems have many advantages, such as prolonged circulation, cell-specific targeting, immune escape, lower toxicity, and better biocompatibility.[30] Red blood cells (RBCs), with a lifespan of about 120 days and many markers on their surface, are considered a biomimetic prototype for developing drug delivery systems based on the RBC-derived membranes (RBCM). The prolonged circulation lifetime of RBC-coated nanosystems is mainly due to diverse membrane proteins such as CD47. After coating with RBCM, the inner nanostructures gain well encapsulation and self-recognition, thus avoiding the phagocytosis of immune cells and prolonging their circulation time.

Recently, Liang *et al.* reported the development of novel stealth and matrix metalloproteinase 2 (MMP2)-activated biomimetic nanosystems against NSCLC, which are constructed using MMP2-responsive peptides to bind miR-126-3p (known as MAIN), and further camouflaged with RBCM (thus named REMAIN). Liang *et al.* demonstrated that REMAIN could effectively transduce miRNA into NSCLC cells and release the cargo through MMP2 responsiveness. The advantages of the natural RBCM mentioned above, such as prolonged circulation, cell-specific targeting, and immune escape, were observed in REMAIN. Furthermore, *in vitro* and *in vivo* results showed that REMAIN effectively induced apoptosis of NSCLC cells and inhibited NSCLC progression by targeting ADAM9.[31] Interestingly, Zhang *et al.*[32] reported an integrated hybrid nanosystem named Clip-PC@CO-LC NPs to specifically target NSCLC, which fused cancer cell membranes (Cm) and matrix metallopeptidase 9 (MMP-9)-switchable peptide-based charge-reversal liposome

Table 1 Administration routes employed in NSCLC using nanoparticles

Administration routes	Nanoparticles	Results	Year and ref.
Intravenous administration	Radioactive ^{153}Sm encapsulated multi-walled carbon nanotubes ($^{153}SmCl_3$@MWCNTs-NH_2)	$^{153}SmCl_3$@MWCNTs-NH_2 showed improved water dispersibility for intravenous administration, high accumulation in site-specific NSCLC tissues, and no leakage of the encapsulated radioactive material for targeted radiotherapy	2021 (ref. 37)
	Mesenchymal stem cell membranes (MSCs)-engineered Fe(III) and cypate-loaded PMAA nanomedicines (Cyp-PMAA-Fe@MSCs)	Cyp-PMAA-Fe@MSCs after intravenous administration were identified 21% higher fluorescence signal and 30% lower T1-weighted MRI signal than Cyp-PMAA-Fe@RBCs, indicating promising application for bioimaging-guided photothermal-enhanced radiotherapy against NSCLC	2021 (ref. 38)
Inhalation	Anti-tumor siRNA-entrapped nanoparticles	Compared with intravenous administration, inhalation administration of the siRNA-loaded nanoparticles showed stronger fluorescent signals in the lung tumor tissues with little systemic toxicity	2019 (ref. 39)
	Silibinin-loaded poly caprolactone/pluronic F68 inhalable nanoparticles (SB-loaded PCL/Pluronic F68 NPs)	Inhalable SB-loaded PCL/Pluronic F68 NPs demonstrated prolonged circulation time, sustained drug release, and excellent NSCLC (A549 cells)-targeting capacity	2022 (ref. 40)
Oral administration	Topotecan-loaded PLGA nanoparticles	Increased bioavailability and prolonged retention of topotecan were found in target organs such as the lung	2021 (ref. 41)
Intraperitoneal administration	Hyaluronic acid-based microRNA-125b encapsulated nanoparticles	Successful repolarization of tumor-associated macrophages was identified in KRAS/p53 double mutant genetically engineered (KP-GEM) NSCLC mice, remarkably improving the efficacy of anticancer immunotherapy	2018 (ref. 42)

membranes (Lipm) to coat lipoic acid-modified polypeptides (LC) co-loaded with phosphoglycerate mutase 1 (PGAM1) siRNA (siPGAM1) and DTX. This nanosystem exhibited a negatively charged coating (citraconic anhydride-grafted poly-L-lysine, PC) in the middle layer for pH-triggered charge conversion functionalization. The use of Cm endowed the final nanosystems with homologous targeting ability, elevated the efficiency of drug delivery to target cells, and boosted the therapeutic effect. Furthermore, in contrast to mono-membrane coating, liposome membranes are more easily modified and can be integrated into a single biomimetic platform to attain various functions for the precise treatment of NSCLC.

2.2. Routes of administration

Given the pivotal role of administration routes in the site-specific accumulation of drugs delivered by nanoparticles, which determines the therapeutic efficacy of NSCLC, great efforts have been devoted to the research to seek the best approach and routes to achieve the anticipated outcomes.[33–35] In general, NSCLC-targeted transportation can be implemented through four methods containing inhalation, intravenous (IV), oral, and parenteral (subcutaneous, intraperitoneal, *etc.*) administration, with the first two being preferred.[36] Here, we list recent applications of these administration routes employed in NSCLC using nanoparticles, as shown in Table 1.

2.3. Mechanism of targeting

The targeting mechanism of nanoparticles can be classified as passive and active targeting. Passive targeting of nanoparticles is principally dependent on the enhanced permeability and retention (EPR) effect supported by the permeable blood vessels in tumors in contrast to the normal capillaries. The enhanced permeability allows macromolecules to escape circulation due to the inherent leakiness of the underdeveloped tumor

Table 2 Targeting strategies of nanoparticles categorized by modified ligands in NSCLC

Conjugated ligands	Targeted receptors	Nanoparticles	Results	Year and ref.
Albumin	Albumin-binding protein BM-40	Albumin liposomes loaded with PD-L1 and siRNA	Albumin liposomes showed efficient accumulation in lung tumor cells	2022 (ref. 45)
Hyaluronic acid	Glycoprotein CD44	CD44 targeting hyaluronic acid-conjugated nanoparticles entrapping microRNA-125	Hyaluronic acid-conjugated nanoparticles exert their strength in site-specific accumulation in mouse models mimicking NSCLC compared to non-targeted nanoparticles or the free drug	2018 (ref. 42)
Folate	Folate receptors	Paclitaxel-loaded folic acid-modified PLGA nanoparticle with glutathione	Due to the high affinity of folate to the receptors, enhanced intracellular uptake of the particles by NSCLC cells was observed, boosting the cytotoxicity of the free paclitaxel or the paclitaxel-entrapped particles without the targeting ligand	2021 (ref. 46)
Transferrin	Transferrin receptors	Transferrin-conjugated protein-lipid hybrid nanoparticles delivering cisplatin and docetaxel (Tf-CIS/DTX-PLHN)	Tf-CIS/DTX-PLHN showed prolonged circulation time, increased drug accumulation, and improved antitumor activity in A549 cells-injected mice compared to non-targeted CIS/DTX-PLHN or free CIS/DTX	2021 (ref. 47)
Aptamer	Complementary DNA or RNA	Aptamers-modified fluorescent superparamagnetic microparticles were paired with the complementary DNA conjugated Au nanoparticles, generating fluorescence resonance energy transfer (FRET) magnetic aptamer-based targeting sensors named Fe3O4@Au	Fe_3O_4@Au, using aptamers as targeting ligands specifically binding to CD63, exhibited efficient capture of NSCLC exosomes, which reached as high as 91.5% with a dosage of 200 μL	2021 (ref. 48)
Monoclonal antibodies	Protein biomarkers (EGFR, HER2, *etc.*)	EGFR antibody conjugated gold nanorods stimulated by pulsed lasers	*In vitro* experiments with NSCLC cells (A549), EGFR antibody modified nanorods exhibited enhanced attenuation of 93% ± 13% in the cell viability compared with untargeted nanorods	2020 (ref. 49)
Peptide fragments (*e.g.* arginine-glycine-aspartic acid (RGD))	Integrin αv β3 as receptors of RGD	Integrin αvβ3-targeted RGD-modified liposomes delivering doxorubicin (DOX)	RGD-modified liposomes exhibited increased cellular uptake and resultant targeted delivery of DOX, leading to enhanced suppression of tumor growth in mice and less toxicity compared with non-RGD functionalized liposomes	2021 (ref. 50)

vasculature. Besides, the lack of an efficient lymphatic system results in the retention of those macromolecules in the tumor bed. Generally, to capitalize on the EPR effect a drug carrier must be in a narrow size range from about 10 nm to 100 nm. Entities smaller than 10 nm are rapidly cleared by the kidneys or through extravasation and larger entities (~100–200 nm) are cleared by the reticuloendothelial system.[20,43] Therefore, nanosystems with suitable size (~10–100 nm) are allowed to extravasate in the tumor tissues, thus achieving NSCLC-targeted drug delivery.

Active targeting is realized through the functionalization of the surface of nanoparticles. Peculiar ligands-conjugated nanoparticles permit a selective recognition of distinguished antigens overexpressed in the NSCLC cell surfaces, improving the therapeutic efficacy of nanoparticles. Based on the category of ligands, active targeting can be divided into various groups including albumin, hyaluronic acid, folate, transferrin, aptamer, monoclonal antibodies, and peptide fragment-based targeting, as shown in Table 2.[44]

On the other hand, according to the targeted goal of NSCLC cells, active targeting can also be classified as tumor microenvironment-targeted, NSCLC biomarkers-targeted, organelles-targeted, and genes or epigenetics-targeted strategies. Extensive applications of these four kinds of targeting strategies are shown in Table 3.

3. Overview of nanosystems

3.1. Lipid-based nanosystems

3.1.1 Liposomes. Liposomes (Fig. 1A) are synthetic spherical delivery vesicles with an amphiphilic lipid bilayer structure consisting of phosphatidylcholine, cholesterol, *etc.*, which will spontaneously assemble when getting scattered in the solution.[58–60] The dominant advantage of this nanocarrier is the capacity to carry both hydrophobic and hydrophilic drugs with the former embedded in the lipid bilayer, while hydrophilic drugs entrapped in the aqueous core, as shown in Fig. 1A.[61] The phospholipid bilayer membranes-like structures make them an

Table 3 Targeting strategies of nanoparticles categorized by a targeted goal in NSCLC

Targeting strategies	Nanoparticles	Results	Year and ref.
Tumor microenvironment-targeted	Hypoxia-responsive nitro-benzyl conjugated chitosan nanoparticles (HRCNs)	HRCNs rapidly determine the hypoxic status of lung cancer cells (A549) within 30 min compared to the conventional method needing several hours, indicating a potential role in the diagnosis and treatment of NSCLC.	2016 (ref. 51)
	GSH-responsive and pH-responsive cisplatin prodrug and paclitaxel co-loaded nanoparticles (DDP-P/PTX NPs)	High tumor accumulation, pH-triggered drug release, low systemic toxicity, and remarkable antitumor effects were observed by DDP-P/PTX NPs in NSCLC-bearing mice	2021 (ref. 52)
Biomarkers -targeted	CD44-targeted, indocyanine green-paclitaxel-loaded albumin nanoparticles	CD44-targeted NPs achieved image-guided drug delivery, exhibiting selective accumulation in CD44-positive NSCLC compared to the normal CD44-negative lung fibroblast cell line (MRC-5)	2022 (ref. 53)
	EGFR-targeted nanoparticles encapsulated erlotinib and quercetin (EQNPs)	*In vivo* experiments showed EQNPs promoted the uptake of nanoparticles in the cancer cells of resistant NSCLC-bearing mice compared to non-targeted NPs. Furthermore, downregulation of nuclear EGFR, improved uptake of Ertb and Quer and induced apoptosis were demonstrated in resistant A549 cells	2022 (ref. 54)
Organelles-targeted	Mitochondria-targeted nonyl acridine orange (NAO)-loaded gold nanorods (NAO-AuNRs)	NAO-AuNRs conjugated with monoclonal antibody Cetuximab have demonstrated their ability in increasing the uptake of the membrane mitochondria-targeted nanomedicine compared to non-targeted ones in NSCLC cells, accompanied by reduced progression of EGFR-positive NSCLC	2022 (ref. 55)
Genes or epigenetics-targeted	βIII-tubulin and polo-like kinase 1 (PLK1)-targeted star polymer-siRNA nanoparticles	The star-siRNA nanoparticles were found accumulated in mouse lung tumors mimicking NSCLC, leading to the silencing of the expression of βIII-tubulin and PLK1 as well as inhibited tumor growth	2022 (ref. 56)
	PEG-PLA hybrid nanocarriers (HNCs) entrapped with cisplatin caprylate and ABCC3-siRNA	ABCC3-siRNA was utilized to specifically target and silence ABCC3 mRNA. Compared with cisplatin solution and cisplatin-loaded HNCs without ABCC3-siRNA, *in vitro* cellular uptake level was increased and cell viability of A549 cells was significantly reduced in the co-loaded nanocarriers, along with a higher rate of cell arrest in G2-M phase	2021 (ref. 57)

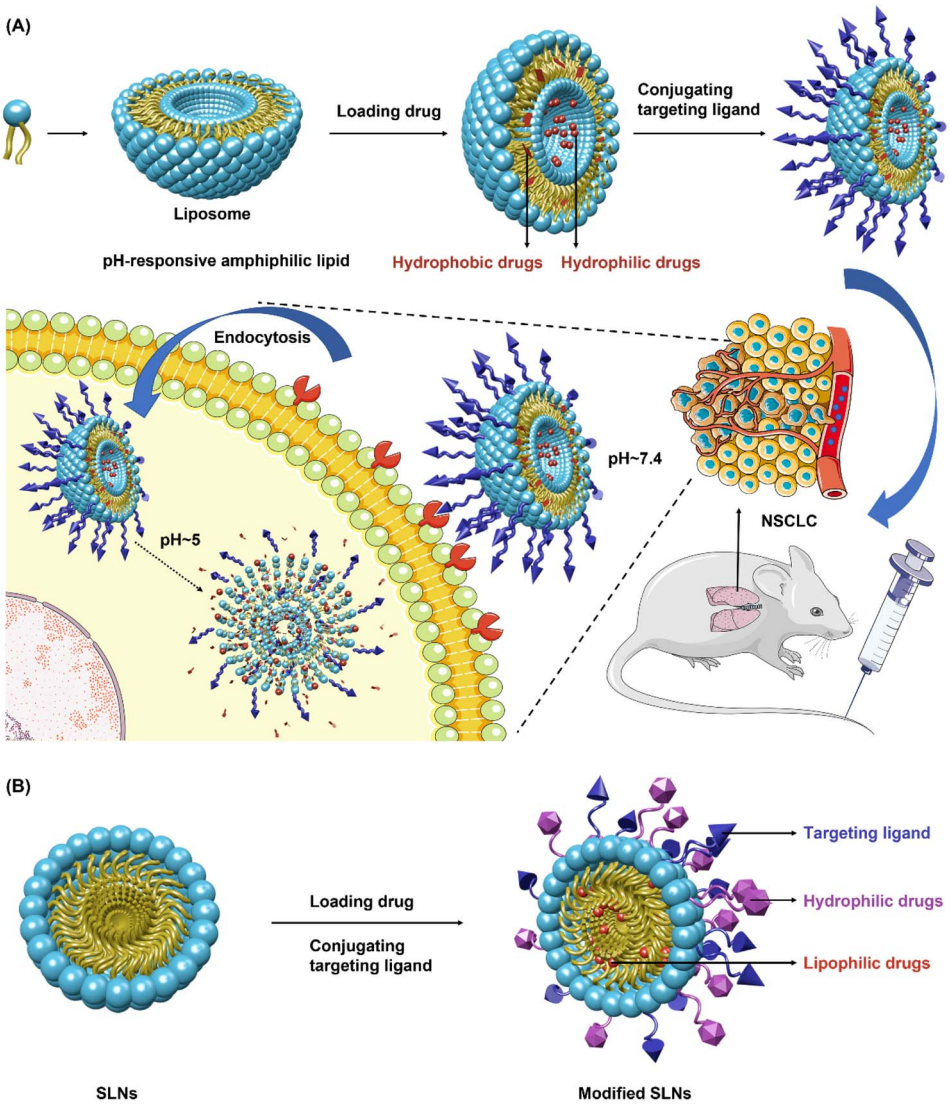

Fig. 1 Lipid-based nanoparticles. (A) Liposomes are spherical nanocarriers with an amphiphilic lipid bilayer structure consisting of phosphatidylcholine, cholesterol, *etc.*, which will spontaneously assemble when getting scattered in the solution. They can carry both hydrophobic and hydrophilic drugs with the former embedded in the lipid bilayer, while hydrophilic drugs entrapped in the aqueous core. Targeting ligand-modified liposomes with pH-responsive amphiphilic lipid allow NSCLC-targeted drug release, which is triggered by intracellular pH. (B) Solid lipid nanoparticles (SLNs) have a close relationship with liposomes but feature much higher drug-loading capacity. SLNs usually consist of solid lipids with the drug either loaded on the surface or entrapped inside the cavity. Their structures generally compromise a solid hydrophobic core coated with a monolayer or multilayer of phospholipid known as an emulsifier, with the core carrying the lipophilic drug. NSCLC, non-small-cell lung cancer. The picture was drawn with Maxon Cinema 4D 25.

efficient drug delivery system due to the advantage of biocompatibility, weak immunogenicity, and biodegradability.[62] Liposomes are usually coated with peptides, enabling them to target a specific site of the body. Meanwhile, using the polymer (β-amino ester) as the outer layer of liposomes facilitates pH-controlled drug delivery for cancer treatment, which also realizes targeted therapy.[63]

3.1.2 Solid lipid nanoparticles (SLNs). SLNs (Fig. 1B), having a close relationship with liposomes described above but featuring much higher drug loading capacity, are colloidal nanocarriers with a diameter ranging from 50 nm to 1000 nm and are constructed using scattering melted solid lipid in emulsifier-added water.[64–66] It was first introduced as an effective and promising alternative in 1991 to make up for deficiencies of emulsions, liposomes, and polymeric systems, representing a more excellent vehicle for drug delivery.[67] SLNs usually consist of solid lipids with the drug either loaded on the surface or entrapped inside the cavity. Their structures generally compromise a solid hydrophobic core coated with a monolayer or multilayer of phospholipid known as an emulsifier, with the core containing the dissolved or dispersed drugs. The hydrophilic chains of phospholipids are present on the shell of the sphere, ensuring dissolution in an aqueous solution, while the hydrophobic segment of the phospholipid embedded into

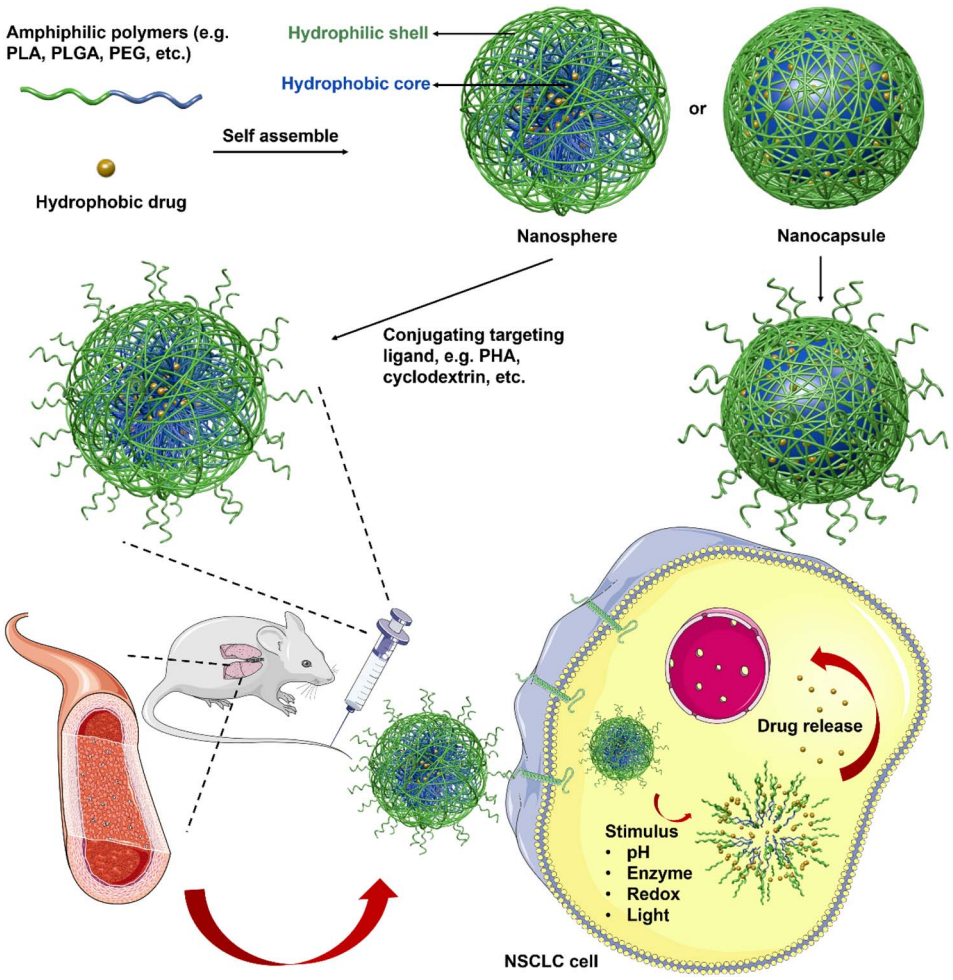

Fig. 2 Polymeric nanoparticles (PNPs). PNPs, which have a core–shell structure comprise nanocapsules and nanospheres. Nanocapsules consist of an oily core with the drug dissolved, coated by a polymeric shell controlling drug release from the core, whilst nanospheres are composed of a continuous polymeric network with the drug contained inside or adsorbed onto the surface. PNPs composed of amphiphilic polymers conduct hydrophobic interaction-mediated self-assembly upon polymers dispersing in the aqueous solution, allowing hydrophobic drugs to be entrapped into the PNPs. The shell can be decorated with polyhydroxyalkanoates, poly(lactic-*co*-glycolic acid), cyclodextrin, and so forth to enable precise targeting. Also, specific moieties-modified PNPs can realize controlled drug release triggered by pH, enzymes, redox, or light. PLA, poly-lactic-acid; PLGA, poly-lactic-acid-*co*-glycolic acid; PEG, polyethylene glycol; PHA, polyhydroxyalkanoates. The picture was drawn with Maxon Cinema 4D 25.

the adipose matrix, acquiring the ability to carry the lipophilic drug, as shown in Fig. 1B.[68] Compared to other colloidal nanocarriers, SLNs do not contain an organic solvent, which is economically feasible for reducing the burden of mass production and render better protection to the encapsulated drug.[69]

3.2. Polymer-based nanosystems

3.2.1 Polymeric nanoparticles (PNPs). PNPs, including nanocapsules and nanospheres (Fig. 2), are core–shell structure nanoparticles with polymers such as poly-lactic-acid-*co*-glycolic acid (PLGA), poly-lactic-acid (PLA), polyethylene glycol (PEG), chitosan, and polycaprolactone.[70,71] Nanocapsules consist of an oily core within the therapeutic drug usually dissolved, coated by a polymeric shell controlling the drug release from the core, whilst nanospheres are composed of continuous polymeric network with the drug contained inside or adsorbed onto the surface.[72] PNPs, composed of amphiphilic polymers, conduct hydrophobic interaction-mediated self-assembly upon polymers dispersing in the aqueous solution, allowing hydrophobic drugs to be entrapped into the PNPs *via* covalent bonding.

3.2.2 Polymer micelles (PMs). PMs (Fig. 3) are self-assembly products of block copolymers with the core–shell structure consisting of a hydrophobic core surrounded by a hydrophilic shell.[73–75] The core of PMs permits to entrap hydrophobic and amphiphilic drugs, allowing controlled drug release, while the shell can prevent the intake of PMs by the RES, prolonging the PMs blood circulation time, which will further increase the drug accumulation in the tumor sites.[76] Upon the concentration of block copolymer molecules surpassing the critical micelle concentration (CMC), they spontaneously assemble into nanoparticles.

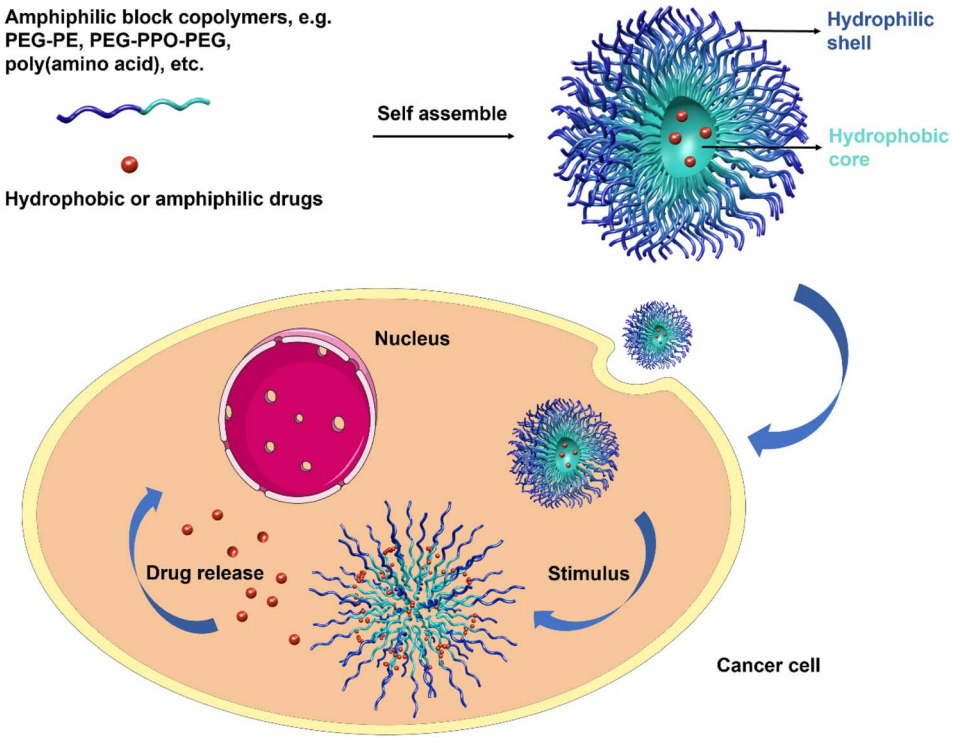

Fig. 3 Polymer micelles (PMs). PMs are self-assembly products of block copolymers with the core–shell structure consisting of a hydrophobic core surrounded by a hydrophilic shell. The core of PMs permits to entrap hydrophobic and amphiphilic drugs, allowing controlled drug release, while the shell can prevent the intake of PMs by the RES, prolonging the blood circulation time of PMs, which will further increase the drug accumulation in the tumor sites. When encountering intracellular or external stimuli such as pH, enzyme, redox, laser, *etc.*, PMs will disassemble to release the drug. PEG, poly(ethylene glycol); PE, phosphatidylethanolamine; PPO, polyphenylene oxygen. The picture was drawn with Maxon Cinema 4D 25.

3.2.3 Dendrimers. Dendrimers (Fig. 4) are a specific type of polymeric nanoparticles featuring a multi-branched 3D structure and modified by multifunctional groups on the surface, which permit to encapsulate or conjugating anti-tumor drug on the surface or in the core, thus significantly improving their functionality and making them versatile.[77–79] Dendrimers are composed of a central core covalently linked by branches of highly repeating units and terminal chemical structures that configure the surface of the dendrimers.[80] Controlled drug release is achieved by the outer functional groups with modifications that are triggered by a certain pH or specific enzymes. Other advantages such as high-degree branches, polyvalency, available internal cavities, and uncomplicated synthesis technology make dendrimers promising agents for applications of diagnosis and therapy.[81]

3.3. Inorganic nanosystems

Generally, inorganic nanosystems can be divided into two groups consisting of metallic nanosystems including gold and silver, and non-metallic nanosystems including iron oxides, carbon nanotubes, silica, selenium (Se), metallic chalcogenide and metallic oxides.[82,83]

3.3.1 Gold Nanoparticles (AuNPs). AuNPs, remotely controlled by NIR, are stable colloid solutions of Au atom clusters with diverse shapes containing gold nanospheres, nanorods, nanocages, nanoshells, and nanostars (Fig. 5A).[68] Attributed to the special properties such as high surface area to volume ratio, ease of synthesis, surface plasmon resonance, easily-modified surface and easy penetration and accumulation of drugs at the tumor tissues, AuNPs are widely utilized for imaging and therapy of various cancers.[84,85] On one hand, AuNPs can be employed as drug delivery systems that simultaneously transport imaging agents and therapeutic drugs to realize both diagnosis and treatment. On the other hand, considering their unique optical and electronic features known as surface plasmon resonance, which causes strong absorption and scattering properties, AuNPs themselves can be used as biosensors for fluorescence imaging triggered by NIR, and as photothermal therapeutic agents that produce cell-killing heat by laser irradiation (Fig. 5B).

3.3.2 Supermagnetic iron oxide nanoparticles (SIONs). SIONs (Fig. 6A) are typically composed of iron oxide cores (γ-Fe_2O_3 orFe_3O_4) coated with a protective material such as chitosan, dextran, PEG, and polyvinyl alcohol (PVA), which permits conjugate with desired moieties (*i.e.*, therapeutic agents, targeting ligands), thereby realizing NSCLC-specific drug delivery.[86,87] Due to their peculiar optical and magnetic properties, SIONs have attracted much attention in laser-induced thermotherapy, MRI, radiotherapy, and photodynamic therapy (PDT).[88] Also, with a large surface area-to-volume ratio, SIONs are endowed with good drug-loading capacity either by

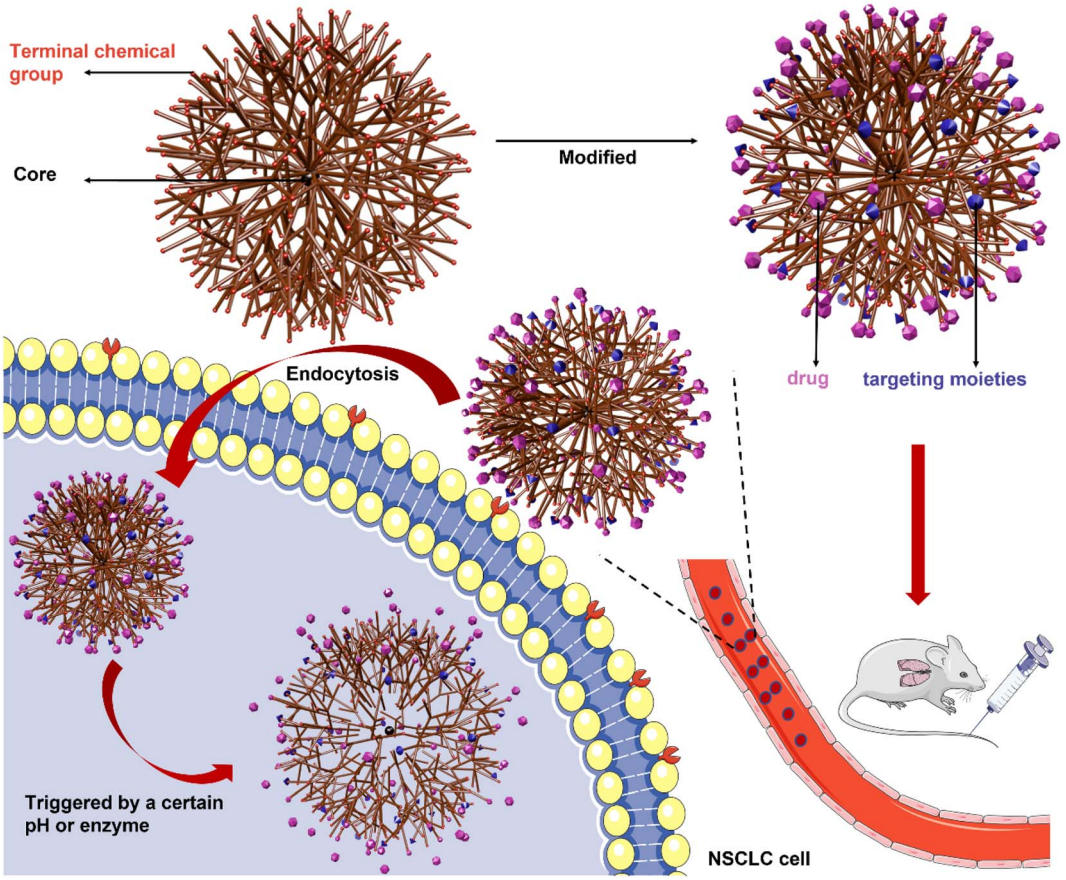

Fig. 4 Dendrimers. Dendrimers are a specific type of polymeric nanoparticles featuring multi-branched 3D-structure and modified by multi-functional groups on the surface, which permit encapsulation or conjugation of anti-tumor drugs on the surface or in the core. They are composed of a central core covalently linked by branches of highly repeating units and terminal chemical structures that configure the surface of the dendrimers. Controlled drug release is achieved by the outer functional groups with modifications that are triggered by a certain pH or specific enzymes. The picture was drawn with Maxon Cinema 4D 25.

conjugating the drug onto the surface or embedded in the coating material. Meanwhile, the shell of SIONs is indispensable in shielding aggregation, and oxidation as well as providing a site for the conjugation of targeting ligands, which also reduces RES-caused clearance in blood circulation.[89]

3.3.3 Carbon nanostructures. Carbon nanostructures such as carbon dots (C-dots), graphene, carbon nanotubes (CNTs), *etc.*, have been stimulating the interest of researchers working on applications for NSCLC diagnosis and therapeutics. Graphene is a two-dimensional material with unique physical and chemical properties such as high electrical and thermal conductivity, mechanical strength, and optical absorption properties. Possessing delocalized π electrons and high surface area render graphene interaction with various biomolecules, which can be used in drug/gene delivery, tissue engineering, and biosensing.[90] C-dots are zero-dimensional discrete spherical nanocarriers with a diameter of less than 10 nm. There are currently two types of C-dots: amorphous-based C-dots (A-C-dots) and graphene-Q-dots (G-Q-dots). A-C-dots are formed by the synchronized sp^2 and sp^3 hybridization of carbon probes, with the ability to surface engineer these molecules further. G-Q-dots have an sp^2-hybridized nanocrystalline carbon core, an asymmetrical configuration that results from the large number of N and O moieties that interrupt the carbonic framework.[91] C-dots have many fascinating properties including strong optical absorption, high fluorescent effects, excellent phosphorescence, outstanding photoluminescence as well as quantum yield, making C-dots promising candidates for cellular imaging, biosensing, and targeted drug delivery.

CNTs have a cylinder-structure third allotrophic form of carbon fullerene consisting of graphene sheets that roll up into an open or capped cylinder.[92–94] Generally, CNTs can be divided into two forms: single-walled carbon nanotube (SWCNT) and multi-walled carbon nanotube (MWCNT) (Fig. 6B). SWCNT, which gains more flexibility attributed to van der Waals forces, is constituted by a single sheet of graphene rolled up to form a tube, while MWCNT comprised of several graphene sheets surrounding one layer of graphene rolled into a tube.[95] Owing to their unique characteristics such as nano-needle shape, hollow monolithic structure, high surface area, extremely light weight, and surface functionalization, CNTs are growing in popularity as one of the most promising nanocarriers.[96] Moreover, CNTs enter cells using "needle-like penetration" and deliver

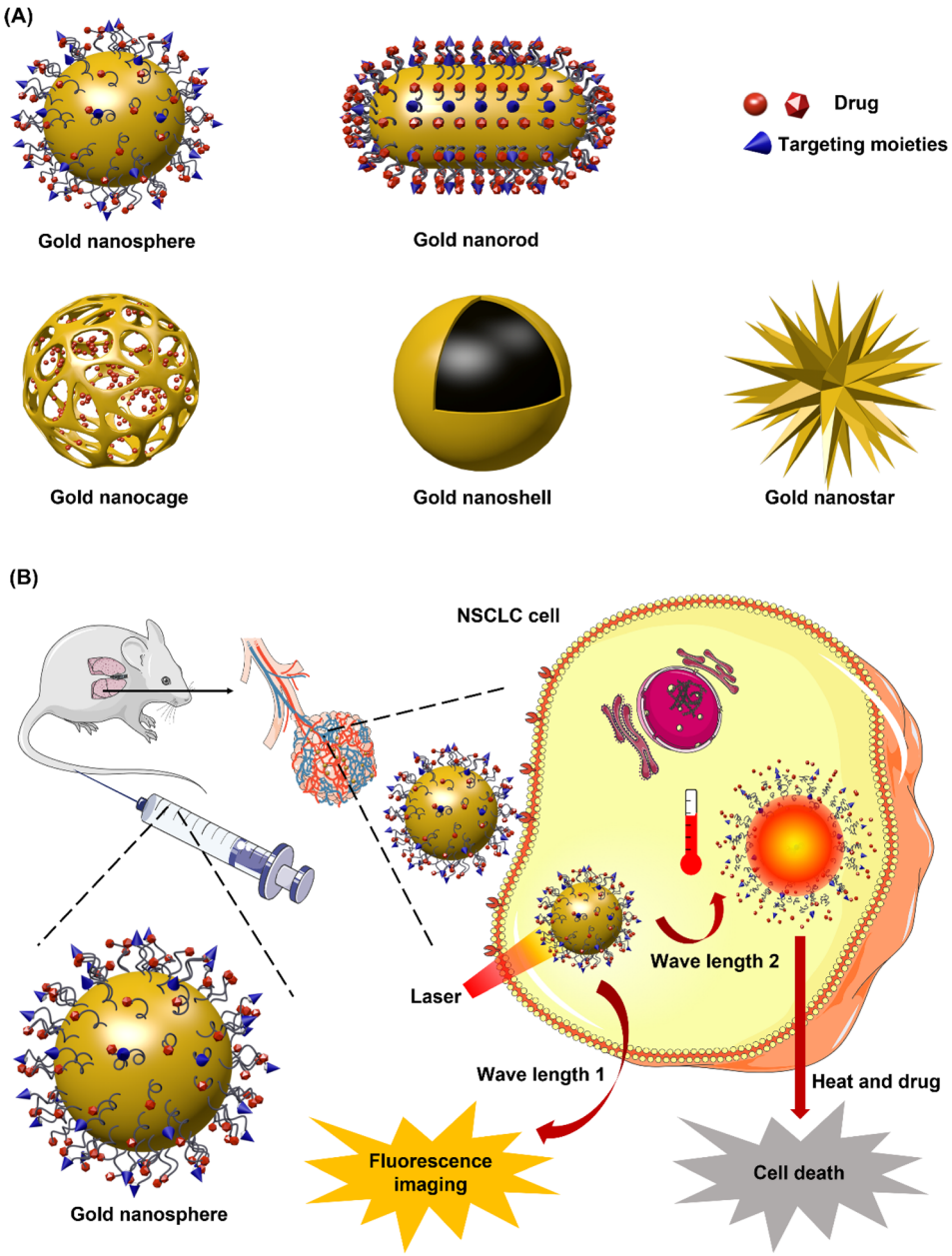

Fig. 5 Gold Nanoparticles (AuNPs). AuNPs are stable colloid solutions of Au atom clusters that are remotely controlled by near-infrared light (NIR). (A) AuNPs have diverse shapes containing gold nanospheres, nanorods, nanocages, nanoshells, and nanostars. (B) AuNPs can be employed as drug delivery systems to transport imaging agents and therapeutic drugs for both diagnosis and treatment, as bio-sensors for fluorescence imaging triggered by NIR, and as photothermal therapeutic agents which produce cell-killing heat by laser irradiation. The picture was drawn with Maxon Cinema 4D 25.

molecules into the cytoplasm, thus further improving the efficiency of drug accumulation.[9]

3.3.4 Mesoporous silica nanoparticles (MSNs). MSNs (Fig. 6C) usually possess a diameter ranging from 50 nm to 200 nm with tightly packed mesopores of size in a range of 3–4 nm.[97–99] MSNs are composed of silicon dioxide and are used widely in applications including synthetic processes, medical diagnosis, and therapy due to their high surface area, tuneable pore size, huge loading capacity, and tailored mesoporous structure. Moreover, the outward surface can be functionalized with "molecular gates", permitting cargo delivery to be triggered by external stimuli such as specific pH, enzymes, and lasers of peculiar wavelengths.[100,101]

4. Nanosystems for NSCLC diagnosis

4.1. Lipid-based nanosysytems

Lipid-based nanosystems have been successfully used for NSCLC diagnosis. Badea *et al.*[102] investigated the utility of a liposomal-iodinated nanoparticle contrast agent and CT

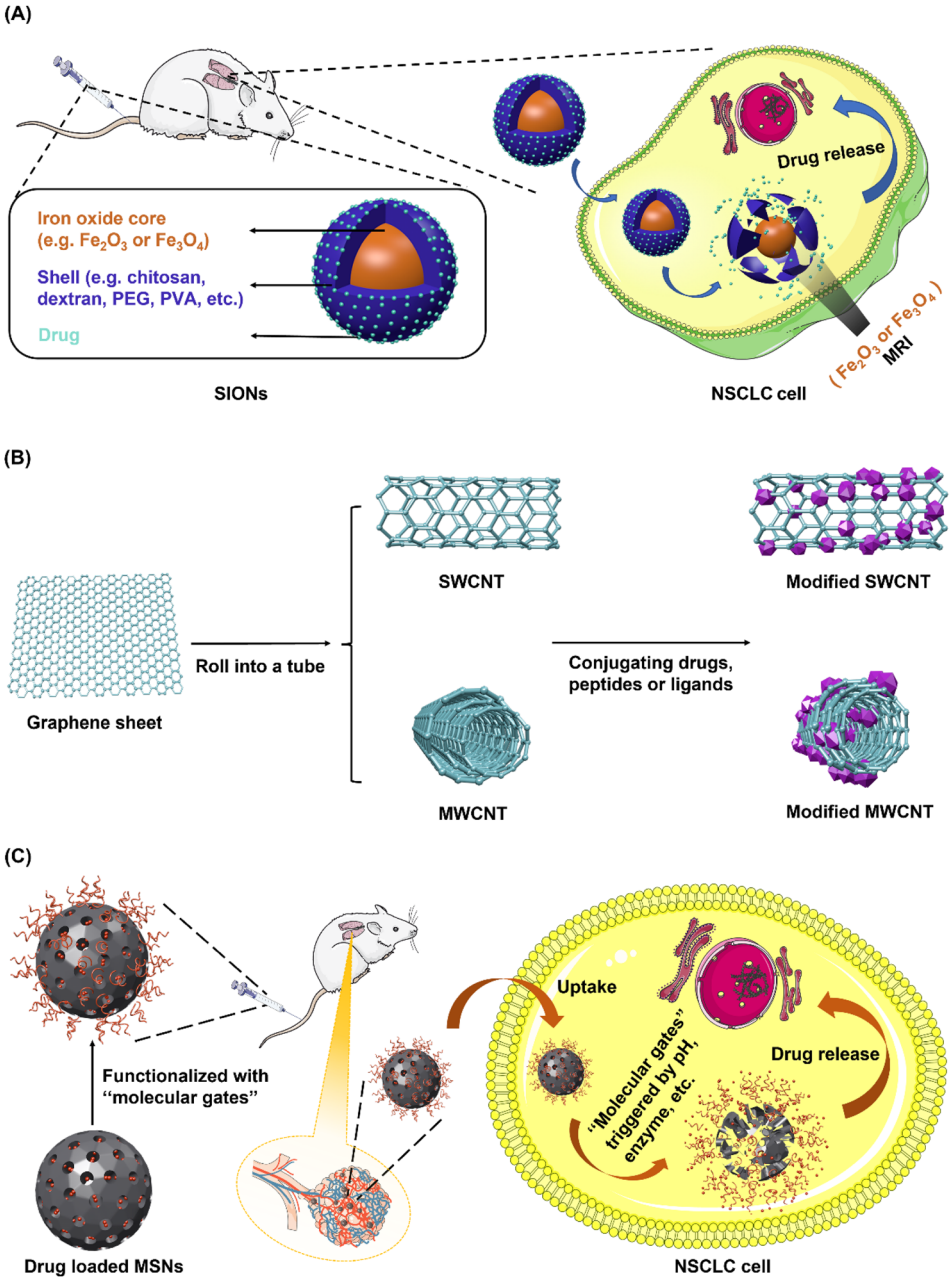

Fig. 6 Non-metallic inorganic nanoparticles. (A) Supermagnetic iron oxide nanoparticles (SIONs) are composed of iron oxide cores coated with protective material, which permits conjugate with desired moieties. Iron oxide cores used for MRI enable SIONs to achieve imaging-guided therapy. MRI, magnetic resonance imaging; PEG, polyethylene glycol; PVA, polyvinyl alcohol. (B) Carbon nanotubes (CNTs), consisting of graphene sheets, can be divided into two forms: single-walled carbon nanotubes (SWCNT) and multi-walled carbon nanotubes (MWCNT). The surface of CNTs can be functionalized with therapeutic drugs or targeting ligands. (C) Mesoporous silica nanoparticles (MSNs), with a diameter ranging from 50 nm to 200 nm with tightly packed 3–4 nm mesopores, are composed of silicon dioxide. The surface can be functionalized with "molecular gates", permitting cargo delivery to be triggered by specific pH, enzyme, and lasers of peculiar wavelengths. The picture was drawn with Maxon Cinema 4D 25.

imaging for the characterization of primary nodules in genetically engineered mouse models of NSCLC. The resultant nanosystem enabled visualization of blood supply to the nodules during the early-phase imaging. Delayed-phase imaging enabled the characterization of slow-growing and rapidly-growing nodules based on signal enhancement. This agent could facilitate the early detection and diagnosis of pulmonary lesions as well as have implications on the treatment response and monitoring.

Exon 2 deletion in aminoacyl tRNA synthetase complex-interacting multifunctional protein 2 (named AIMP2-DX2) has been suggested to be associated with the progression of various cancers such as lung cancer. Jo *et al.*[103] demonstrated the rapid and simple detection of the AIMP2-DX2 mutation by molecular

beacons and its relation to lung cancer. Real-time PCR with molecular beacons allowed sensitive detection of the AIMP2-DX2 mutation as low as 0.3 pg initial template. Dual-conjugated liposomes with folate and molecular beacons enabled fluorescence imaging of cancer cells harboring the AIMP2-DX2 mutation with high resolution. The association of the AIMP2-DX2 mutation with lung cancer was shown by analyzing tissue samples from lung cancer patients using real-time PCR. Approximately, 60% of lung cancer patients harbored the AIMP2-DX2 mutation, which implies a potential of the AIMP2-DX2 mutation as a prognostic biomarker for lung cancer. This study indicated that molecular beacon-based liposomes had great potential in the simple and rapid detection of mutations on nucleotides for diagnosing and monitoring the progression of relevant cancers.

4.2. Polymer-based nanosystems

Macromolecular contrast agents were first investigated for MR angiography (MRA) considering that the conventional low molecular weight gadolinium (Gd)(III) agents fail to offer vessel opacification times sufficient to allow MR imaging. Compared with conventional agents that exhibit rapid equilibration with the extravascular extracellular space (EES) and are rapidly cleared by renal filtration, macromolecular agents exhibit extended vascular retention times, a critical property for MR imaging.[104]

Among these macromolecular agents, dendrimers are promising nanosystems used for NSCLC imaging. Two types of dendrimers have been widely explored as imaging agents, one type within the poly(propyleneime) (PPI) dendrimer series, composed of a 1,4-diaminobutane (DAB) core, the other of the poly(amidoamine) (PAMAM) dendrimer series composed of a 1,2-diaminoethane core. The defined structures and availability of the surface amino groups of dendrimers enable the development of dendrimer-conjugates with various chelates for the application as MR contrast agents.[105,106] Zhu *et al.*[107] built Lox-Stop-lox K-ras G12D transgenic mice imitating lung cancer. It was found that miR-155 and somatostatin receptor 2 (SSTR2) were expressed in all the disease stages of transgenic mice. The authors synthesized octreotide-conjugated chitosan-molecular beacon nanoparticles (CS-MB-OCT) that can specifically bind to SSTR2 expressed by the lung cancer cells to achieve the goal of identification of lung cancer cells and imaging miR-155 *in vivo* and *in vitro*. Fluorescence imaging at different disease stages of lung cancer in the transgenic mice was performed, and could dynamically monitor the occurrence and development of lung cancer by different fluorescence intensity ranges. This research provided new ideas, new methods, and new technology for the early screening of lung cancer.

4.3. Inorganic nanosystems

4.3.1 AuNPs. AuNPs have been extensively investigated as radio-opaque contrast agents, replacing the traditional iodinated molecules dissolved in liquids.[108] Furthermore, gold-coated nanoshells are prospective optical imaging agents given their tunable plasmon resonance, which enables them to be specifically designed to match the wavelength desired for a peculiar use. AuNPs currently in use vary in size, involving 1.9 nm in diameter for X-ray contrast, ≤40 nm in diameter for gold–gold sulfide nanoshells, as well as 50–500 nm in diameter for silica-gold core–shell nanoshells.[109,110] Barash *et al.* in 2012 put forward a nanodevice for the classification of lung cancer (LC) histology, which permits to discriminate between (i) LC and healthy cells; (ii) SCLC and NSCLC; and between (iii) two subtypes of NSCLC: adenocarcinoma and squamous cell carcinoma. Owing to the fact that the fabricated nanodevice had the competence of profiling volatile organic compounds (VOCs) in the headspace of LC cells through gas chromatography-mass spectrometry analysis, the discrimination and diagnosis of lung cancer were achieved.[111] In a recently published report by Hu *et al.*, the authors introduced a sensitive electrochemical immunosensor named AuNPs@MoS_2@Ti_3C_2Tx composites for monitoring NSCLC through detecting marker Cytokeratin fragment antigen 21-1 (CYFRA21-1). In this study, AuNPs were modified using Ti_3C_2Tx and molybdenum disulfide (MoS_2), thus acquiring great surface area and splendid electrocatalytic characteristics. The detection boundary could reach as low as 0.03 pg ml^{-1} within the concentration of CYFRA21-1 ranging from 0.5 pg ml^{-1} to 50 ng ml^{-1} in which the electrochemical response value increased linearly.[112]

4.3.2 SIONs. Magnetic nanoparticles have been well explored as MRI contrast agents and have huge potential for drug-delivery tracking. Generally, there are two types of magnetic nanoparticles employed in medical imaging: one is SIONs with a mean hydrodynamic diameter (HD) of >50 nm, involving the feruxomides (Endorem [Guerbet Villepinte, France] or Feridex IV [Advanced Magnetics, Cambridge, MA], the other is ultrasmall SIONs (USIONs) with an HD <50 nm, such as Ferumoxtran-10 (Advanced Magnetics, Cambridge, MA).[113] Park *et al.*, in 2020 synthetized ^{64}Cu-labeled folate-conjugated SIONs for positron emission tomography (PET)/MRI-based diagnosis of cancer. The new type of SIONs showed excellent performance in lung (A549) cancer cell lines. Radio-thin-layer chromatography (TLC) analysis showed that SIONs with a radiochemical purity of 82.17% and stability of ~90% in human serum for 24 h.[114]

4.3.3 Carbon nanostructures. There is vast interest in the application of carbon nanostructures such as C60 fullerenes and CNTs in NSCLC imaging, which have been proven as prospective contrast agents. Advantages of carbon nanostructures include enhanced relaxivity compared with conventional contrast agents (when loaded with Gd(III)), an outer carbon sheath that is readily functionalized for targeting, an excellent track record of biocompatibility, and favorable lipophilicity and size for crossing cell membranes for intracellular accumulation.[115] In the field of MR imaging, Gd(III)-loaded metalofullerenes, or gadofullerenes, exhibit the potentiality to be a new generation of higher-performance contrast agents. Constraint of the Gd(III) within the fullerene cage avoids dissociation of toxic Gd ions *in vivo*, thus declining the risk of toxicity.[116,117] Besides, specifically derivatized Gd C60 nanomaterials, with diameters of 1 nm, have been demonstrated to have 20 times more relaxivity than conventional MRI agents.[118]

However, clinical use of these carbon nanostructures has been impeded by their RES accumulation and spontaneous aggregation *in vivo* (observed with polyhydoxylated fullerene derivatives).[115] In view of these issues, water-soluble formulations excreted by the kidney have been investigated. *In vivo* behavior of soluble Gd@C60 derivative, namely Gd@C60[C(COOH)2]10 gadofullerenes, was assessed and these derivatives exhibited declined RES uptake and enhanced urinary excretion.[119] Altogether, the development of a fullerene MR contrast agent excreted by the kidney represents a significant step in the progress of clinically feasible carbon nanostructure-based contrast agents.

SWNTs are also emerging as a potent type of nanosystems for molecular imaging. Given their relative ease of synthesis compared with metallofullerenes and the significantly huger relaxivity realized by gadolinium-based SWNT contrast agents compared with conventional contrast agents, SWNT-based contrast agents may show prominent progress for MRI. Also, their intrinsic near-infrared fluorescence enables SWNTs to be prospective optical agents.[115] Aasi *et al.* introduced SWCNTs decorated by platinum–group transition metals (Pt, Pd, Rh, or Ru) as potential nanosensors for the detection of toluene, an important biomarker in the exhaled breath of the lung cancer patients. It was observed that toluene is intensely chemisorbed on Rh- and Ru-SWCNT systems with the ascendant response (−96.98% and −99.98%, respectively), and moderately chemisorbed on Pt-SWCNTs (−27.3%) and Pd-SWCNTs (61.60%), testifying metal decorated SWCNTs sensors as attractive candidates for the early detection of NSCLC.[120]

4.3.4 MSNs. MSNs are promising optical imaging agents, ranging from a few nanometers to over 100 nm in diameter. Merits of MSNs involve great emission intensity, exceptional photostability, water solubility, an easily modifiable surface as well as tunable pore sizes, thus making MSNs an ideal platform for MR-enhancing hybrid materials. MSNs loaded with Gd(III) have been developed as effective MR contrast agents. Altogether, the development of porous nanosystems that permit access of water molecules to magnetic cores is a crucial step in the progress of nanoscale contrast agents for MR imaging.[121] Kang *et al.*[122] reported a nanosystem named carbon dot (CD) created mesoporous hollow organosilica (C-hMOS) nanoparticles, to deliver anticancer drugs and to enable optical imaging. The hollow structure was formed by the removal of the nanorod core template, and at the same time, the fluorescent signal was endowed by the heat-treated organosilica network. The treatment of C-hMOS in cancer cells enabled multi-color visualization *in vitro*, suggesting the possibility of cell tracing. Moreover, when injected intratumorally in mice, C-hMOS exhibited strong optical signals *in vivo* along with high optical stability (over a week), making it a promising nanoplatform for drug delivery and *in vivo* imaging in cancer treatment.

Herein, we summarize all the above-mentioned studies of nanosystems for NSCLC diagnosis, as shown in Table 4.

Notably, in standard practice, the US Food and Drug Administration demands that agents administered for diagnostic purposes must be cleared completely from the body within a reasonable time period. Longmire *et al.* suggested that renal filtration was the ideal route for nanomedicine removal from the body, and nanosystems with size <6 nm and zwitterionic or cationic surface charge may be optimized to boost renal clearance. Clearance of metal-containing nanosystems is particularly significant owing to agent toxicity and the likelihood of interference with other diagnostic imaging modalities. For instance, metal nanosystems may interfere with X-ray imaging owing to changes in linear attenuation coefficient, MRI owing to proton-free voids, ultrasound owing to enhanced echogenicity, and probably even single photon emission computed tomography and PET owing to photon attenuation.[17,115]

5. Nanosystems for NSCLC treatment with/without image guidance

As mentioned above, nanotechnology has revolutionized the use of carriers for treating NSCLC, which are described in detail in the following sections. Apart from summarizing the recent application of lipid-based nanosystems, polymer-based nanosystems, and inorganic nanosystems against NSCLC, we additionally introduce vaccine and gene delivery nanosystems given their increasingly important role as novel approaches for NSCLC treatment.

5.1. Lipid-based nanosysytems

5.1.1 Liposomes. Gai *et al.*[123] prepared folate (FA)-modified liposome (FA-LP) nanoparticles for targeted co-delivery of erastin and MT1DP to increase the bioavailability and the efficiency of the drug/gene combination. The resultant nanosystems called Erastin/MT1DP@FA-LPs (E/M@FA-LPs) sensitized erastin-induced ferroptosis with decreased cellular GSH levels and elevated lipid ROS. *In vivo* analysis demonstrated that E/M@FA-LPs had a favorable therapeutic effect on lung cancer xenografts. Their study identified a novel strategy to elevate erastin-induced ferroptosis in NSCLCs acting through the MT1DP/miR-365a-3p/NRF2 axis. Recently, Zhang *et al.*[32] investigated the role of cancer cell membrane-hybrid liposomes triggered by tumor microenvironment in synergistic metabolic therapy and chemotherapy against NSCLC. The liposomes entitled CLip-PC@CO-LC NPs had hybrid nanovesicles comprised of cancer cell membranes (Cm) and liposome membranes (Lipm) activated by matrix metallopeptidase 9 (MMP-9) as the shell, while lipoic acid-modified polypeptides (LC) loaded with phosphoglycerate mutase 1 (PGAM1) siRNA (siPGAM1) and DTX were entrapped in the core. It was found that CLip-PC@CO-LC NPs displayed the traits of pH-controlled membrane disruption and redox-responsive DTX and siRNA release, thus resulting in highly robust glycolysis-related gene silencing and enhanced antiproliferation ability of chemotherapy.

Though liposomes are widely utilized for NSCLC theranostics, challenges still lie in the variation between batch to batch, expensive mass production cost, induced pro-inflammatory cytokines, possible drug leakage, *etc.*[124] Nevertheless, some functionalized liposomes have entered the

Table 4 Summary of discussed studies on nanosystems for NSCLC diagnosis

Nanocarrier	Imaging agent	Targeting group	Advantages	Drawbacks	Ref.
Liposome	Iodinated-liposome	—	This nanosystem enabled the visualization of blood supply to the nodules during the early-phase imaging. Delayed-phase imaging enabled the characterization of slow-growing and rapidly-growing nodules based on signal enhancement	The routine analysis is challenging in rodent studies due to small feature size and high noise levels on micro-CT scanners	102
Liposome	Molecular beacon detecting AIMP2-DX2 mutation	Folate	Simple and rapid detection of mutations on nucleotides for diagnosing and monitoring the progression of relevant cancers	Lack of *in vivo* studies and toxicity assessment	103
Chitosan PNPs	miR-155 molecular beacon	Octreotide (OCT)	Fluorescence imaging at different disease stages of lung cancer in transgenic mice could dynamically monitor the occurrence and development of lung cancer	Lack of toxicity assessment	107
AuNPs	Organic ligands provided broadly cross-selective adsorption sites for the breath VOCs	—	These nanosensors are suitable for detecting lung cancer (LC) specific patterns of volatile organic compounds (VOCs) profiles, allowing early differential diagnosis of LC subtypes	Lack of *in vivo* studies and toxicity assessment	111
AuNPs	Ti_3C_2Tx and MoS_2	—	The detection boundary can reach as low as 0.03 pg ml^{-1} within the concentration of CYFRA21-1 ranging from 0.5 pg ml^{-1} to 50 ng ml^{-1}	Lack of toxicity assessment	112
SIONs	^{64}Cu and Fe_3O_4	Folate	This nanosystem yielded good radiochemical purity of 82.17% without the presence of a free 64Cu mobile phase and exhibited ~90% stability in both buffer solution and human serum for 24 h, making it a potential nanoprobe for PET/MRI-based diagnosis of NSCLC.	Lack of *in vivo* studies and toxicity assessment	114
Metallofullerene	Gd	—	Avoided RES accumulation and spontaneous aggregation *in vivo* as a promising MRI contrast agent	Lack of toxicity assessment	119
SWCNTs	SWCNTs and platinum-group transition metals (Pt, Pd, Rh, or Ru)	—	Attractive candidates for the detection of toluene, a lung cancer biomarker in the exhaled breath of lung cancer patients	The lack of reversibility originated from the strong chemical reaction between the toluene and the metal atom	120
C-dot-induced hollow mesoporous organosilica nanocarriers	Carbon dot and silica	—	Enabled multi-color visualization *in vitro*, and exhibited strong optical signals *in vivo* along with high optical stability (over a week)	Can be further explored with modifications such as targeting moiety and PEGylation	122

clinical stage, herein we summarize main examples of liposomal formulations in clinical trials (Table 5).

5.1.2 SLNs. Bae and co-workers[130] designed quantum dots and paclitaxel-loaded SLNs conjugating Bcl-2 targeted siRNA on the surface for *in situ* NSCLC imaging-guided synergistic chemotherapy. The resultant nanocomplexes were observed with powerful fluorescence derived from quantum dots and efficient transportation of paclitaxel and siRNA in specific sites of lung tumor tissues. Furthermore, the authors found improved synergistic anticancer activities of the SLN/siRNA nanomedicine in a manner of caspase-mediated apoptosis, suggesting that the optically traceable SLN is a potential alternative to imaging-guided therapy of NSCLC. Interestingly, Yang *et al.*[131] reported an inhaled microspheres system that co-delivers afatinib and paclitaxel (PTX) for the treatment of EGFR TKIs resistant NSCLC. In this system, afatinib was loaded in stearic acid-based SLNs, then, these nanoparticles and PTX were loaded in poly-lactide-*co*-glycolide-based porous microspheres. Cell experiments indicated that afatinib and PTX had a synergistic effect and the codelivery system showed a superior treatment effect in drug-resistant NSCLC cells. The biocompatibility, pharmacokinetic, and tissue distribution

Table 5 Liposomal formulations in clinical trials

Product name	Composition	Clinical phase	Clinical use	Clinical trials (https://clinicaltrials.gov) identifier or ref.
L-BLP25 (Stimuvax®)	MUC1-targeted liposome vaccine	Phase III	Unresectable stage III NSCLC	NCT00157196 (ref. 125)
Lipoplatin	Liposome encapsulated formulation of cisplatin	Phase II	Metastatic NSCLC	NCT00006036 (ref. 126)
OTAP: Chol-fus1	DOTAP:cholesterol liposomal nanoparticles complexed with a plasmid expression cassette encoding human FUS1 protein	Phase I	Advanced NSCLC	NCT00059605
ATRC-101	Pegylated liposomal doxorubicin (PLD)	Phase IB	Advanced solid malignancies containing NSCLC, breast cancer, colorectal cancer, ovarian cancer, *etc.*	NCT04244552
ATI-1123	Liposomal docetaxel formulation	Phase I	Solid tumors including NSCLC and breast cancer	NCT01041235
STM 434	Liposomal doxorubicin	Phase I	Solid tumors such as NSCLC, ovarian cancer, fallopian tube cancer, endometrial cancer	NCT02262455
MM-310	EphA2 receptor-targeted liposomal formulation of a docetaxel prodrug	Phase I	NSCLC, solid tumors, urothelial carcinoma, gastric carcinoma, squamous cell carcinoma of the head and neck, *etc.*	NCT03076372
MnSOD	Manganese superoxide dismutase (MnSOD) plasmid liposome (PL)	Phase I	Advanced stage III NSCLC	NCT00618917 (ref. 127)
Aroplatin (L-NDPP)	Liposomal formulation of *cis*-bis-neodecanoato-*trans*-*R*,*R*-1,2-diaminocyclohexane platinum(II)	Phase II	NSCLC, advanced colorectal cancer	128
SPI-77	Sterically stabilized liposomal cisplatin	Phase II	Advanced NSCLC	129

experiments in Sprague-Dawley rats showed that afatinib and PTX in the system could maintain 96 h of high lung concentration but the low concentration in other tissues, with acceptable safety. These results demonstrated that this system may be a prospective delivery strategy for drug combination treatment in drug-resistant NSCLC.

However, similar to other colloidal nanocarriers, SLNs suffer rapid elimination from circulation for the sake of the reticular endothelial system (RES), thus resulting in limited drug delivery. In addition, a significant challenge occurring in the drug-loading process is the dissolution of drug molecules into lipids.[132]

5.2. Polymer-based nanosystems

5.2.1 PNPs. In 2021, Yin and colleagues developed a new type of PNPs entitled Cyp-PMAA-Fe@MSCs comprised of polymethacrylic acid (PMAA) coated by mesenchymal stem cell membranes (MSCs) PNPs carrying Fe(III) and cypate, which was a derivative of indocyanine green, to realize fluorescence/MRI bimodal imaging and imaging-guided photothermal therapy-enhanced radiotherapy against NSCLC. *In vivo* experiments demonstrated that the tumor site-specific fluorescence signal in the Cyp-PMAA-Fe@MSCs group was 21% stronger compared to that in the Cyp-PMAA-Fe@RBCs group after intravenous injection into tumor-bearing mice. Consistently, the T1-weighted MRI signal was 30% weaker in the Cyp-PMAA-Fe@MSCs group at the lung tumor sites. Furthermore, the Cyp-PMAA-Fe@MSCs showed excellent manifestation in photothermal cell-killing effect both *in vitro* and *in vivo* when irradiated by 808 nm laser, indicating it is a potential prospect for diagnosis and imaging-guided combined treatment of NSCLC.[38] Very recently, to provide a prospective treatment of EGFR-TKI-resistant NSCLC, Huang *et al.*[133] proposed a nano-cocktail therapeutic strategy by exploiting stimuli-responsive dendritic-polymers loaded with EGFR-TKI gefitinib (Gef) and yes-associated protein (YAP)-siRNA to enable targeted drug/gene/photodynamic therapy. The cocktail PNPs were observed to efficiently internalize into resistant NSCLC cells avoiding lyolysis from lysosomes, the intracellular pH-triggered release of Gef and YAP-siRNA, and no distinguished toxicity after laser irradiation. In this study, blockage of the EGFR signaling pathway *via* Gef, suppression of EGFR bypass signaling pathway with YAP-siRNA, and increased apoptosis of tumor cells was achieved in a stimuli-responsive drug release manner, proving that the cocktail PNPs are predatory competitors compared with pure photodynamic therapy or free drug therapy. However, there is still a challenge lying in the large-scale production considering the complicated synthesis processing, thus asserting a claim for more research and advance in this aspect.

5.2.2 PMs. In 2020, DTX-loaded *N*-(*tert*-butoxycarbonyl)-L-phenylalanine end-capped methoxy-poly (ethylene glycol)-block-poly (D,L-lactide) (mPEG-*b*-PLA-Phe(Boc)) micelles (DTX-

PMs) were designed by Gong *et al.*, showing better aqueous solubility, stability, and lower toxicity. In the *in vivo* study in human NSCLC (A549) tumor-bearing Balb/c nude mice, DTX-PMs were found to considerably enhance DTX accumulation, and achieve better therapeutic efficacy.[134] Interestingly, Wang *et al.*[135] synthesized a novel folate conjugated poly(ethylene glycol)-poly(L-glutamic acid)-poly(L-phenylalanine) (folate-PEG-PLG(HS)-PPhe) copolymer to achieve a desired controlled delivery of DOX. The copolymer could self-assemble into interlayer-crosslinked micelles with reduction sensitivity, and DOX was successfully loaded into the interior of the copolymer. The interlayer-crosslinked disulfide bond at the intermediate region between PEG and poly(L-phenylalanine) resulted in significant improvement of the system stability through the introduction of an additional mechanism of carrier/carrier interaction. The crosslinked interlayer could be cleaved at the desired target site under tumor-relevant reductive conditions and DOX was rapidly released from the DOX-loaded folate-PEG-PLG (HS)-Pphe micelles (DOX-fPGPM), and significantly lowered the drug leakage without glutathione (GSH). Importantly, the DOX-fPGPM exhibited significantly higher antitumor efficiency both *in vitro* and *in vivo* in comparison with free DOX, and Doxil (commercial doxorubicin-loaded liposomes). The DOX-fPGPM designed in this work could potentially resolve the dilemma between systemic stability and rapid intracellular drug release and would provide a promising nanomedicine platform for cancer therapy.

However, disadvantages including leakage of the encapsulated drug during the delivery, weak solubility of small-sized micelles, and limited loading competence are still persecuting reseachers.[75]

5.2.3 Dendrimers. Zhu and colleagues, in 2021, designed and synthetized aptamer-modified fluorinated dendrimer called APFHG co-delivering gefitinib (Gef) and photosensitizer hematoporphyrin (Hp) to alleviate hypoxia and overcome the resistance of EGFR-TKIs-based molecular targeted therapy combined with photodynamic therapy against NSCLC. The aptamer-modified fluorinated dendrimer (APF) had excellent oxygen-carrying ability, high drug entrapment efficiency, and controlled release of Gef and Hp triggered by intracellular pH. APFHG could greatly promote the production of intracellular reactive oxygen species (ROS) and amplified the therapeutic effect.[136] However, the limitation of structural defects owing to the terminal functional group leads to deficiency in the stoichiometrical reaction. In another study, Maghsoudnia *et al.*[137] investigated the anti-tumor effect of microRNA Mimic let-7b loaded in PAMAM dendrimers (G5) on NSCLC. Chloroquine was also employed to enhance the endosomal escape. PAMAM dendrimers were coated with "hyaluronic acid (HA)" to develop biodegradable carriers with targeting moiety for over-expressed CD44 receptors on NSCLC cells. Remarkably, the dendrimers in the cells pretreated with chloroquine exhibited the highest cytotoxicity and were capable of inducing apoptosis. Moreover, the expression study of three genes linked with cancer initiation and development in NSCLC, including KRAS, p-21, and BCL-2 indicated a decrease in KRAS and BCL-2 (oncogenic and anti-apoptotic genes) and an increase in p-21 (apoptotic gene). This study declared that the application of let-7b-loaded PAMAM-HA NPs in combination with chloroquine can be a promising therapeutic option in cancer cell inhibition.

Extensive applications of polymer-based nanoparticles containing PNPs, PMs, and dendrimers that have entered clinical trials are shown in Table 6.

5.3. Inorganic nanosystems

5.3.1 AuNPs. Peng *et al.*, in 2021, developed Au-RGD-miR-320a nanoparticles for directly targeting Sp1 in NSCLC. A new type of gold nanorods were modified with polyethyleneimine and endowed with RGD peptide-mediated peculiar targeting ability, which condensed miRNA to self-assemble to the supramolecular nanostructure. The therapeutic action of the designed nanoparticles was constituted by integrin αvβ3-targeted therapy, laser irradiation-responsive photosensitive therapy, and miRNAs-mediated gene-targeted therapy, which eventually repressed the proliferation and metastasis, and promoted the apoptosis of lung cancer through upregulated the expression of PTEN and downregulated the expression of matrix metallopeptidase 9.[143] Very recently, Ma *et al.*[144] fabricated a nanosystem of gold nanoparticles-dextran nanoparticles loaded with hypoxia-activated paclitaxel dimeric prodrug nanoparticles (PTX2-NP) and photosensitizer chlorin e6/paclitaxel-nanoparticle/gold@N-(2-hydroxypropyl) (Ce6/PTX2-NP/G@NHs) and analyzed the possible molecular mechanism for enhancing the radiosensitivity of NSCLC. Ce6/PTX2-NP/G@NHs were effectively internalized by A549 cells, producing cytotoxicity under laser irradiation. The resultant nanosystem reduced cell viability, clonogenic potential, migration, and invasion along with ROS production while promoting apoptosis in A549 cells under laser irradiation. By inhibiting the PI3K/AKT pathway, this nanosystem increased the sensitivity of A549 cells to radiotherapy where apoptotic body (ApoBD)-mediated neighboring effects also played a key role.

5.3.2 SIONs. Recently, Ngema and colleagues reported the synthesis of *trans*-10, *cis*-12 conjugated linoleic acid (CLA)-coated SIONs delivering paclitaxel (PTX), which were proven to amplify anti-proliferative activity on the A549 lung cancer cells with a cell viability of 17.1%. The CLA-coated PTX-SIONs showed a drug loading efficiency of 98.5% and persistent site-specific release of PTX *in vitro* over 24 h, thus suggesting that the nanomedicine is a promising alternative for an effective drug delivery system targeted NSCLC.[145] Interestingly, Qin *et al.*[146] designed a hybrid nanosystem (SIONs + RPPs) in which phase transition nanodroplets with immunomodulatory capabilities were used to potentiate SION-mediated mild magnetic hyperthermia (MHT, <44 °C) and further inhibit tumour proliferation and metastasis. Magnetic-thermal sensitive phase-transition nanodroplets (RPPs) were fabricated from the immune adjuvant resiquimod (R848) and the phase transition agent perfluoropentane (PFP) encapsulated in a PLGA shell. Because of the cavitation effect of microbubbles produced by RPPs, the temperature threshold of MHT could be lowered from 50 °C to approximately 44 °C with a comparable effect, enhancing the release and exposure of damage-associated

Table 6 Polymer-based nanoparticles in clinical trials

Product name	Composition	Clinical phase	Clinical use	Clinical trials (https://clinicaltrials.gov) identifier or ref.
CRLX101 (NLG207)	Cyclodextrin and camptothecin loaded polymer nanoparticle	Phase II	Advanced NSCLC, advanced solid tumor malignancies	NCT01380769 (ref. 138)
Genexol-PM	Cremorphor EL (CrEL)-free polymeric micelle formulation of paclitaxel	Phase II	Advanced NSCLC	NCT01770795 (ref. 139)
NC-6004	Polymeric micelle formulation of cisplatin	Phase I/II	Advanced unresectable NSCLC, biliary tract, or bladder cancer	NCT02240238 (ref. 140)
NC-4016	1,2-Diaminocyclohexane platinum(II) (DACHPt)-incorporating micelles	Phase I	Various solid tumors	NCT03168035 (ref. 61)
NC-6300	Epirubicin-incorporating micelle	Phase IB	Advanced solid tumors including NSCLC, soft tissue sarcoma, metastatic sarcoma, sarcoma	NCT03168061 (ref. 141)
BIND-014	PSMA-targeted docetaxel-containing polymeric micelle	Phase I	Advanced solid tumors including NSCLC	NCT02283320 (ref. 142)
XMT-1001	Camptothecin (CPT) conjugated Fleximer®	Phase I	Non-small cell lung cancer, small cell lung cancer	NCT00455052

molecular patterns (DAMPs). The exposure of calreticulin (CRT) on the cell membrane increased by 72.39%, and the released high-mobility group B1 (HMGB1) increased by 45.84% *in vivo*. Moreover, the maturation rate of dendritic cells (DCs) increased from 4.17 to 61.33%, and the infiltration of cytotoxic T lymphocytes (CTLs) increased from 10.44 to 35.68%. Under the dual action of mild MHT and immune stimulation, contralateral and lung metastasis could be significantly inhibited after treatment with the hybrid nanosystem. Collectively, this study provided a novel strategy for enhanced mild magnetic hyperthermia immunotherapy and ultrasound imaging with great clinical translation potential.

5.3.3 Carbon nanostructures. Augustine *et al.*[147] recently designed oxidized graphene nanoribbons (O-GNRs)-based delivery system for cisplatin against NSCLC cell line A549 by selective endocytosis. The nanoformulation showed an average inhibition of 22.72% at a lower dose of cisplatin (>25%) by passive targeting on cell line A549 by DNA alkylation, indicating that graphene-based systems were potential nanosystems against NSCLC. In another study, Ahamed *et al.*[148] certificated the therapeutic efficacy of combining SWCNTs with ubiquitous cadmium (Cd) against NSCLC is of tremendous satisfaction. Unavoidable side effects of Cd, such as induced cell viability reduction, reactive oxygen species, and cell cycle arrest were remarkably abrogated by joint effects of SWCNTs in human lung epithelial (A549) cells.

5.3.4 MSNs. Recently, a versatile nanocomposite heterogeneous platform was put forward by Lin *et al.* for therapeutic alliance against NSCLC, which implied the synthesis of folic acid-mediated MSNs@Ag@Geb. The large surface area empowered the MSNs heterostructure the competence to efficiently load photothermal agents Ag and chemotherapeutic agents Geb, which were pH-responsive drug release achieved by degradation of residual MnO_2.[149] Wu *et al.*[150] formulated a novel MSNs loaded with PDLIM5 siRNA. The results showed that PDLIM5 siRNA could be effectively bound to the nanoplatforms and had good biocompatibility. Further exploration suggested that the nano-platform combined with ultrasonic irradiation could be very effective for siRNA delivery and ultrasound imaging. Moreover, epithelial-mesenchymal transformation (EMT) changes occurred in PC-9 Gefitinib resistance (PC-9/GR) cells during the development of drug resistance. When PDLIM5 siRNA entered PC-9/GR cells, the sensitivity of drug-resistant cells to gefitinib could be restored, indicating that this nanoplatform may become a novel treatment for EGFR TKIs resistance in NSCLC patients.

5.4. Vaccine delivery nanosystems

Cancer vaccines that elicit a specific cytotoxic immune response to tumor antigens are a promising strategy for NSCLC immunotherapy. A major obstacle to developing a novel NSCLC vaccine is the successful and effective delivery of NSCLC antigens to specific cell populations, NK cells, and antigen-presenting cells (APCs). Antigens are relatively fragile in the blood microenvironment and readily susceptible to degradation. Employing nanosystems as delivery systems is a prospective way to address ineffective antigen delivery.

Liposome-based NSCLC vaccines have been advanced into clinical studies. Tecemotide (L-BLP25) is a MUC1 glycoprotein immunotherapy liposomal vaccine combined with MPLA, which is capable of inducing antigen-specific T-cell responses.[151] This vaccine formulation was demonstrated to induce a dominant Th1 response and CTL specific to MUC1. Interestingly, Butts *et al.*[125] carried out a phase III trial and found no significant difference in overall survival with the administration of L-BLP25 after chemoradiotherapy compared with a placebo for all patients with unresectable stage III NSCLC. Therefore, more liposomal vaccine studies are worth conducting depending on the stage of NSCLC relative to the treatment regimen employed. Parayath *et al.* utilized hyaluronic

acid nanoparticles loaded with microRNA-125b to reprogram M2 phenotype MØs in an NSCLC murine model. These nanoparticles were observed to target CD44+ MØs and modified to enable negatively charged nucleotide encapsulation.[152] The repolarization of tumor-associated MØs to M1 phenotype was testified by altered surface biomarker expression.

These studies suggested that nanosystems are promising vectors for antigen delivery in the NSCLC vaccine. Nanovaccines can reduce the dose and number of immunizations for many vaccines, provide rapid and long-lived immunity in a single dose, activate humoral and cell-mediated immunity, allow room temperature storage for long periods of time, and enhance patient compliance. However, challenges that still need to be overcome include translation from lab to clinic, scale-up costs, and regulatory approvals.

5.5. Gene delivery nanosystems

The efficient delivery of the nucleic acid gained attention to its target tissue and nanocarriers. Generally, the exogenous genetic material must be delivered to the nucleus of the targeted cells, where they manufacture the protein products of the introduced gene. The ideal vector transfers a precise amount of genetic material into a specific cell type that achieves the level and duration of transgene expression sufficient to correct the defect and be non-immunogenic and harmless, allowing expression of the gene product without causing toxicity.[153] In the following sections, we discuss the advancements of nanocarriers used to deliver miRNA, siRNA, antisense oligonucleotides, and plasmid DNA for NSCLC treatment.

5.5.1 miRNAs. The levels of miR-34 and miR-let-7, two tumor-suppressive miRNAs, are significantly decreased in NSCLC tissue.[154,155] Studies have demonstrated that miR-34 is capable of protecting against initiation and progression of $Kras^{G12D+/}$; $p53^{R172H/+}$ lung cancers and human NSCLC xenografts, and exogenous miR-let-7 can suppress Kras-associated lung cancers.[155,156] Wiggins *et al.* used SLN composed of cationic lipids to deliver miR-34a to affect apoptosis in cancer stem cells, however, these cationic lipids resulted in liver toxicity.[157] Encouragingly, neutral lipids have been proven non-toxic carriers for miRNAs, conquering the challenge proposed by cationic lipids. This neutral lipid-based delivery for miR-34a led to a significant accumulation of miRNAs and downregulation of the target genes in NSCLC tissues.[158] In another study, miR-let-7a was encapsulated in modified nanoliposomes, which were conjugated with ephrin-A1 to specifically bind to the highly expressed EphA2 membrane receptors on NSCLC cells. This nanoliposome was observed to obviously inhibit the RAS signaling pathway, hence impeding the proliferation and growth of NSCLC cells.[82] However, there are still challenges to nanosystem-based miRNA delivery existing in their low encapsulation efficiency, poor transfection efficiency, non-specific biodistribution, and systemic clearance.

5.5.2 Small interfering RNAs (siRNAs). Chemically synthesized siRNAs with the desired sequence can be exploited to selectively knock down the expression of specific genes that are critical for the pathophysiology of cancers, such as different signaling pathways involved in cancer cell growth, metastasis, angiogenesis, or drug resistance. This phenomenon is called RNA interference. siRNAs have a net negative charge that deters their entry into the cell and suffers from rapid degradation by RNAases as well as reticuloendothelial system-mediated elimination.[159] These problems can be settled by utilizing nanosystems to deliver siRNAs into specific cells. A study reported a siRNA-delivery system to silence the NSCLC cells, which was called iNOP-7 made up of a highly branched generation of four poly-L-lysine dendrimers consisting of 32 amino acids on its surface. The study showed that NSCLC cell proliferation was evidently decreased by iNOP-7-PLK1 siRNA (polo-like kinase 1 siRNA).[160] Another study indicated that the nanosystems composed of cationic lipid/solid polymer hybrid could be used for siRNA delivery considering that these hybrid nanosystems led to prolonged blood circulation, efficient gene silencing, and minimal *in vivo* side effects.[161]

5.5.3 Antisense oligonucleotides. Antisense oligonucleotides are single-stranded generally ranging from 13 to 25 nucleotides and match with the specific mRNA sequence during the translation process, which further regulates the synthesis of target proteins, thereby providing high selectivity for the target and improving the therapeutic index as compared with other antitumor therapies.[162] Cationic lipid nanoparticles are the most advanced and widely used nanosystems to deliver anionic oligonucleotides.[163] Amreddy *et al.* discussed PLGA nanoparticles, which are cationized with biocompatible chitosan to deliver antisense oligonucleotides. Chitosan-modified PLGA nanoparticles bonded to antisense oligonucleotide 2′-*O*-methyl-RNA were observed for cellular uptake efficiency in NSCLC. The results suggested that the cellular uptake of antisense 2′-*O*-methyl-RNA was up to the percentage of chitosan in the nanoparticles. Moreover, the chitosan-modified nanoparticles were proven to remarkably inhibit the telomerase activity in lung cancer cells.[164]

5.5.4 Plasmid DNA. Genetic mutations such as KRAS and p53 are regularly observed in NSCLC, which declines the responsiveness of treatment against NSCLC. Talekar *et al.*[165] investigated the application of plasmid DNA, wt-p53, which was delivered as a therapeutic biomaterial in SK-LU-1 human lung adenocarcinomas and in the $Kras^{G12D}/p53^{fl/fl}$ genetically engineered mouse model of lung cancer. They utilized hyaluronic acid-based nano vehicles for the systematic delivery of plasmid DNA at the target site, which led to significantly increased apoptotic activity in SK-LU-1 lung cancer cells. The tumor suppressor candidate 2 (*TUSC2,* also called *FUS1*) gene possesses the highest tumor-suppressor activity, but it is not detected in most of the NSCLC cell lines. This gene exhibits the most dynamic proapoptotic activity compared with other tumor-suppressor genes in NSCLC cells. Liposomes of *N*-[1-(2,3-dioleoyloxy)propyl]-*N*,*N*,*N*-trimethylammonium chloride (DOTAP): Cholesterol encapsulating TUSC2-expressing plasmid DNA is proven to be an attractive intravenous gene delivery system in NSCLC. The nano-delivery of TUSC2 plasmid reduced the number of metastatic nodules and increased survival rates in metastasis mouse models.[166]

Table 7 Summary of the discussed on nanosystems for the NSCLC treatment

Nanocarrier	Cargo	Targeting group	Advantages	Drawbacks	Ref.
Liposome	Erastin and MT1DP	Folate	Sensitized erastin-induced ferroptosis with decreased cellular GSH levels and elevated lipid ROS, and showed a favorable therapeutic effect on lung cancer xenografts	—	123
NSCLC cell membrane-hybrid liposome	Lipoic acid-modified polypeptides (LC) loaded with phosphoglycerate mutase 1 (PGAM1) siRNA (siPGAM1) and DTX	NSCLC cell membrane	pH-controlled membrane disruption and redox-responsive DTX and siRNA release, thus resulting in highly robust glycolysis-related gene silencing and enhanced antiproliferation ability of chemotherapy	—	32
SLNs	Quantum dots, paclitaxel and Bcl-2 targeted siRNA	—	Imaging-guided synergistic chemotherapy: this nanosystem showed powerful fluorescence derived from quantum dots and efficient transportation of paclitaxel and siRNA in specific sites of lung tumor tissues	Lack of *in vivo* study and toxicity evaluation	130
SLNs	Afatinib and paclitaxel	—	Showed a superior treatment effect in EGFR TKIs-resistant NSCLC cells	*In vivo* study showed slight liver toxicity, which can recover over time	131
PNPs (PMAA)	Fe(III) and cypate	Mesenchymal stem cell membranes	Realized fluorescence/MRI bimodal imaging and imaging-guided photothermal-therapy-enhanced radiotherapy against NSCLC	Lack of toxicity evaluation	38
PNPs	Gefitinib (Gef) and Yes-associated protein (YAP)-siRNA	—	Achieved a targeted drug/gene/photodynamic therapy against EGFR-TKI-resistant NSCLC.	—	133
PMs	DTX	—	Considerably enhanced DTX accumulation, thus achieving better therapeutic efficacy	—	134
PMs	DOX	Folate	Resolved the dilemma between systemic stability and rapid intracellular drug release	—	135
Fluorinated dendrimers	Gef and hematoporphyrin (Hp)	Aptamer	Greatly promoted the production of the intracellular ROS and amplified the therapeutic effect against EGFR-TKI resistant NSCLC	Lack of *in vivo* study and toxicity evaluation	136
PAMAM dendrimers (G5)	microRNA Mimic let-7b and chloroquine	Hyaluronic acid	Expression study of three genes linked with cancer initiation and development in NSCLC, including KRAS, p-21, and BCL-2, indicated a decrease in KRAS and BCL-2 (oncogenic and anti-apoptotic genes) and an increase in p-21 (apoptotic gene)	Lack of *in vivo* study	137
Gold nanorod	miR-320a	RGD peptide	Achieved integrin αvβ3-targeted therapy, photosensitive therapy by laser irradiation, and gene-targeted therapy by miR-320a	—	143
Gold nanoparticles-dextran nanoparticles	Paclitaxel dimeric prodrug and photosensitizer Ce6	—	Enhanced the radiosensitivity of NSCLC.	—	144
trans-10, *cis*-12 conjugated linoleic acid (CLA)-coated SIONs	Paclitaxel	—	CLA (with potential anticancer activity) could yield a more efficacious nanomedicine for NSCLC chemotherapy with enhanced anti-proliferative activity and biocompatibility	Lack of *in vivo* study and toxicity evaluation	145
Hybrid nanosystem (SIONs + RPPs)	Immune adjuvant resiquimod (R848) and	—	A novel strategy for enhanced mild magnetic hyperthermia	Lack of toxicity evaluation	146

Table 7 (*Contd.*)

Nanocarrier	Cargo	Targeting group	Advantages	Drawbacks	Ref.
	the phase transition agent perfluoropentane (PFP)		immunotherapy and ultrasound imaging with great clinical translation potential		
Oxidized graphene nanoribbons	Cisplatin	—	Showed an average inhibition of 22.72% at a lower dose of cisplatin (>25%) by passive targeting on cell line A549 by DNA alkylation	Lack of *in vivo* study and toxicity evaluation	147
SWCNTs	Cadmium	—	Unavoidable side effects of Cd, such as induced cell viability reduction, reactive oxygen species, and cell cycle arrest were remarkably abrogated by joint effects of SWCNTs in A549 cells	Lack of *in vivo* study and toxicity evaluation	148
MSNs	Ag and Geb	Folic acid	Combined photothermal therapy and molecular targeted therapy, and achieved pH-responsive drug release by the degradation of residual MnO_2	—	149
MSNs	PDLIM5 siRNA	—	Very effective for siRNA delivery and ultrasound imaging, and the sensitivity of drug-resistant cells to gefitinib was restored	—	150
Liposomal vaccine (L-BLP25)	A synthetic 25-amino acid lipopeptide derived from the tandem repeat region of MUC1, and nonspecific adjuvant monophosphoryl lipid A	—	Induced a dominant Th1 response and CTL specific to MUC1 in the study by Mehta *et al.*	A phase III trial found no significant difference in overall survival with the administration of L-BLP25 after chemoradiotherapy compared with a placebo	125,151
Hyaluronic acid-based nanoparticles	miRNA-125b	Hyaluronic acid	Reprogrammed tumor-associated macrophages to overcome immunosuppression	—	152
SLNs	miR-34a	—	Provided a new strategy to deliver miRNA	Liver toxicity	157
Liposome	miR-let-7a	Ephrin-A1	Obviously inhibit the RAS signaling pathway, hence impeding the proliferation and growth of NSCLC cells	—	82
Dendrimers	iNOP-7-PLK1 siRNA	—	A novel strategy for the treatment of NSCLC which aberrantly express PLK1	Lack of toxicity evaluation	160
PNPs (PLGA)	Antisense oligonucleotide 2′-*O*-methyl-RNA	—	Remarkably inhibit the telomerase activity in the lung cancer cells	—	164
PEI/PEG NPs	Wild-type p53 and miR-125b expressing plasmid DNA	Hyaluronic acid (HA)	Showed tremendous promise of wt-p53 and miR-125b gene therapy using dual CD44/EGFR-targeting HA NP vector for effective treatment of lung cancer	Lack of toxicity evaluation	165
Liposome	TUSC2-expressing plasmid DNA	—	Reduced the number of metastatic nodules and increased survival rates in metastasis mouse models	—	166

Herein, we summarize all the above-mentioned studies of nanosystems for NSCLC treatment, as shown in Table 7.

6. Discussion and perspectives

Huynh and Zheng[167] introduced two design concepts for engineering multifunctional nanosystems: a conventional approach called 'all-in-one', and a novel approach called 'one-for-all'. The all-in-one approach means components that own a specific singular function such as a drug or imaging contrast agent are combined, leading to multiple single components packaged in a single nanosystem. This approach is generally achieved by either encapsulating agents within the core, conjugating or adsorbing agents to the surface of the nanosystem, or a combination of these ways, thus making the resultant nanosystem

become increasingly complex with the addition of multiple imaging agents and drugs. On the other hand, one-for-all means a multifunctional nanosystem can be made from a single building block that owns multiple intrinsic functionalities such as being a carrier, drug, and imaging agent, simultaneously. This approach aims to simplify the composition of the multifunctional nanosystem while retaining the required properties. Many inorganic nanosystems have both imaging and treatment feasibility, such as SIONs used for MRI and thermal therapy,[168] AuNPs for CT and radiation therapy,[169] gold nanorods for CT contrast enhancement, and PTT.[170]

Both, all-in-one and one-for-all design approaches, possess merits and demerits. The aspects most remarkably discriminating the two approaches are clinical translation—manufacturing methodologies and presumable toxicity.

The major superiority of the all-in-one approach is the readily available components, many of which are based on materials already utilized in the clinic, thereby reducing challenges related to regulatory approval. However, the inferiority of the all-in-one approach is still troublesome, featuring relatively higher clinical translation hurdles and more complicated toxicity studies. In this approach, the synthesis of multifunctional nanosystems entails the addition of singular functional components in a step-by-step manner, hence demanding multiple purification courses. Accordingly, this synthesis approach is highly time-consuming, and multistep purification usually reduces the final yield, thereby causing expensive scale-up costs and impeding their clinical use. Moreover, presumable heterogeneous formulations may occur due to multiple cargos packaged in one single nanosystem. Although a step-by-step procedure may attenuate the heterogeneity and elevate reproducibility, it will result in increased synthesis time and costs. On the other hand, combining multiple steps is capable of reducing the synthesis steps, but resulting in declined reproducibility and enhanced heterogeneity amongst nanosystems in the same production batch. Moreover, biodistribution, biocompatibility, toxicity, and biodegradation also limit progress towards clinical use, entailing to ponder on each component of the formulation, because many multifunctional nanosystems consist of both organic and inorganic components, which are not cleared from the body in the same manner. Besides, the size of nanosystems also affects the routes of clearance *via* either liver or renal filtration. For this reason, a multifunctional nanosystem with smaller nanoparticles packaged within it may have several routes of clearance, thus demanding complex toxicity studies for multiple components.

As for the one-for-all approach, the major superiority lies in relatively lower clinical translation hurdles and simpler toxicity studies. In this approach, the synthesis procedure of multifunctional nanosystems is simplified because a single building block does not demand complicated fabrication steps, while ensuring a homogenous formulation and only demands biodistribution, biocompatibility, toxicity, and biodegradation studies for the single component. However, most of the multifunctional nanomaterials are inorganic, which poses threats to long-term toxicity and *in vivo* clearance considering that they are not biodegradable. Moreover, inorganic nanomaterials are usually confined to be specific for an individual imaging modality, resulting in finite flexibility for multiple desired therapeutic and imaging functionalities. Besides, the one-for-all approach challenges researchers to synthesize inherently multifunctional building blocks, which will demand their own regulatory approval.

7. Conclusions

Non-small-cell lung cancer (NSCLC) is a devastating disease of high incidence and mortality all over the world. Sensitive diagnosis and effective therapy methods are crucial for alleviating the conditions of patients whose lives are threatened by the disease. Nanoparticles have been established to be tools with enormous benefits and widely applied in the clinic against NSCLC. The structure of nanoparticles can be manipulated and regulated, which permits limitations and problems existing in conventional theranostic treatments to be overcome such as solubility and stability issues through surface chemistry.

Multi-drug resistance (MDR), which has a close relationship with tumor cell heterogeneity, gene mutations, efflux pump, tumor microenvironment, *etc.*, has been a huge obstacle to the long-term therapeutic outcomes of NSCL.[9] Fortunately, nanoparticles have displayed prospective possibilities for overcoming MDR. It is well demonstrated that diverse chemotherapeutic or immunotherapeutic drugs delivered as nanoparticle cargoes are endowed with the ability to bypass MDR partially because drugs delivered by nanocarriers cannot be recognized as substrates by the ABC drug efflux systems.

Although there has been a great deal of research concerning nanoparticles delivering NSCLC drugs, only a handful of such nanomedicine have entered the market. This situation is mainly attributed to the fact that the *in vivo* performance of nanomedicine is of great possibility to be very distinguished from its performance *in vitro*, which has something to do with aspects of cell interactions, tissue transportation, diffusion, and biocompatibility in different settings. Nevertheless, nanoparticles have made great progress over the last decades, and considering the market prospect of nanoparticles against NSCLC, opportunities primarily exist in combination with conventional treatments such as chemotherapeutics, NSCLC-oriented, and patient-featured therapy guidelines.

Author contributions

Piao Jiang and Qinglin Shen: conceptualization, writing—original draft preparation. Piao Jiang, Bin Liang, Zhen Zhang, Quan Xu, Weirong Yao, Qinglin Shen: writing—review and editing. Piao Jiang, Qinglin Shen: Visualization. Bing Fan, Lin Zeng, Zhiyong Zhou, Zhifang Mao: supervision, project administration. Qinglin Shen, Weirong Yao, Quan Xu: funding acquisition. All authors have read and agreed to the published version of the manuscript.

Conflicts of interest

The authors declare no competing financial interest.

Acknowledgements

P. J., B. L., and Z. Z contributed equally to this work. This work was financially supported by the Scientific research projects of the Jiangxi Provincial Health Commission (202130003), the Scientific research projects of the Jiangxi Administration of Traditional Chinese Medicine (2021A370), and the Scientific research projects of the Department of Education of Jiangxi Provincial (GJJ218909).

References

1 J. R. Molina, P. Yang, S. D. Cassivi, S. E. Schild and A. A. Adjei, *Mayo Clin. Proc.*, 2008, **83**, 584–594.
2 Y. Wang, Y. Zhang, Z. Du, M. Wu and G. Zhang, *Int. J. Nanomed.*, 2012, **7**, 2315–2324.
3 C. García-Fernández, C. Fornaguera and S. Borrós, *Cancers*, 2020, **12**, 1609.
4 L. Chang, J. Li and R. Zhang, *Biochim. Biophys. Acta, Rev. Cancer*, 2022, **1877**, 188729.
5 C. Gridelli, A. Rossi, D. P. Carbone, J. Guarize, N. Karachaliou, T. Mok, F. Petrella, L. Spaggiari and R. Rosell, *Nat. Rev. Dis. Primers*, 2015, **1**, 15009.
6 M. E. Daly, N. Singh, N. Ismaila, M. B. Antonoff, D. A. Arenberg, J. Bradley, E. David, F. Detterbeck, M. Früh, M. A. Gubens, A. C. Moore, S. K. Padda, J. D. Patel, T. Phillips, A. Qin, C. Robinson and C. B. Simone, *J. Clin. Oncol.*, 2022, **40**, 1356–1384.
7 P. Chen, Y. Liu, Y. Wen and C. Zhou, *Cancer Commun.*, 2022, **42**, 937–970.
8 M. S. Goldberg, *Nat. Rev. Cancer*, 2019, **19**, 587–602.
9 J. L. Markman, A. Rekechenetskiy, E. Holler and J. Y. Ljubimova, *Adv. Drug Delivery Rev.*, 2013, **65**, 1866–1879.
10 K. Bukowski, M. Kciuk and R. Kontek, *Int. J. Mol. Sci.*, 2020, **21**, 3233.
11 H. K. Sajja, M. P. East, H. Mao, Y. A. Wang, S. Nie and L. Yang, *Curr. Drug Discovery Technol.*, 2009, **6**, 43–51.
12 A. Selmani, D. Kovačević and K. Bohinc, *Adv. Colloid Interface Sci.*, 2022, **303**, 102640.
13 Y. Xu, T. Fourniols, Y. Labrak, V. Préat, A. Beloqui and A. des Rieux, *ACS Nano*, 2022, **16**, 7168–7196.
14 Y. Yang, X. Zheng, L. Chen, X. Gong, H. Yang, X. Duan and Y. Zhu, *Int. J. Nanomed.*, 2022, **17**, 2041–2067.
15 W. He, G. Ma, Q. Shen and Z. Tang, *Nanomaterials*, 2022, **12**, 1738.
16 B. B. Oliveira, D. Ferreira, A. R. Fernandes and P. V. Baptista, *Wiley Interdiscip. Rev.: Nanomed. Nanobiotechnol.*, 2023, **15**, e1836.
17 H. S. Choi, W. Liu, P. Misra, E. Tanaka, J. P. Zimmer, B. Itty Ipe, M. G. Bawendi and J. V. Frangioni, *Nat. Biotechnol.*, 2007, **25**, 1165–1170.
18 S. M. Moghimi, H. Hedeman, I. S. Muir, L. Illum and S. S. Davis, *Biochim. Biophys. Acta*, 1993, **1157**, 233–240.
19 C. J. Porter, S. M. Moghimi, L. Illum and S. S. Davis, *FEBS Lett.*, 1992, **305**, 62–66.
20 R. A. Petros and J. M. DeSimone, *Nat. Rev. Drug Discovery*, 2010, **9**, 615–627.
21 J. D. Byrne, T. Betancourt and L. Brannon-Peppas, *Adv. Drug Delivery Rev.*, 2008, **60**, 1615–1626.
22 J. Chen, Y. Zhang, Z. Meng, L. Guo, X. Yuan, Y. Zhang, Y. Chai, J. L. Sessler, Q. Meng and C. Li, *Chem. Sci.*, 2020, **11**, 6275–6282.
23 H. Kim, K. Chung, S. Lee, D. H. Kim and H. Lee, *Wiley Interdiscip. Rev.: Nanomed. Nanobiotechnol.*, 2016, **8**, 23–45.
24 M. P. Melancon, M. Zhou and C. Li, *Acc. Chem. Res.*, 2011, **44**, 947–956.
25 S. M. Mohamed, S. Veeranarayanan, T. Maekawa and S. K. Dasappan Nair, *Adv. Drug Delivery Rev.*, 2019, **138**, 18–40.
26 P. Zhang, C. Hu, W. Ran, J. Meng, Q. Yin and Y. Li, *Theranostics*, 2016, **6**, 948–968.
27 X. Li, W. Li, M. Wang and Z. Liao, *J. Controlled Release*, 2021, **335**, 437–448.
28 Y. Z. Zhao, L. N. Du, C. T. Lu, Y. G. Jin and S. P. Ge, *Int. J. Nanomed.*, 2013, **8**, 1621–1633.
29 L. Fu and H. T. Ke, *Cancer Biol. Med.*, 2016, **13**, 313–324.
30 Q. Lin, Y. Peng, Y. Wen, X. Li, D. Du, W. Dai, W. Tian and Y. Meng, *Beilstein J. Nanotechnol.*, 2023, **14**, 262–279.
31 L. Liang, H. Cen, J. Huang, A. Qin, W. Xu, S. Wang, Z. Chen, L. Tan, Q. Zhang, X. Yu, X. Yang and L. Zhang, *Mol. Cancer*, 2022, **21**, 186.
32 W. Zhang, C. Gong, Z. Chen, M. Li, Y. Li and J. Gao, *J. Nanobiotechnol.*, 2021, **19**, 339.
33 L. Wang, Y. Rao, X. Liu, L. Sun, J. Gong, H. Zhang, L. Shen, A. Bao and H. Yang, *J. Nanobiotechnol.*, 2021, **19**, 56.
34 P. Graván, A. Aguilera-Garrido, J. A. Marchal, S. A. Navarro-Marchal and F. Galisteo-González, *Adv. Colloid Interface Sci.*, 2023, **314**, 102871.
35 M. B. McGuckin, J. Wang, R. Ghanma, N. Qin, S. D. Palma, R. F. Donnelly and A. J. Paredes, *J. Controlled Release*, 2022, **345**, 334–353.
36 A. K. Thakur, D. K. Chellappan, K. Dua, M. Mehta, S. Satija and I. Singh, *Expert Opin. Ther. Pat.*, 2020, **30**, 375–387.
37 A. Gajewska, J. T. Wang, R. Klippstein, M. Martincic, E. Pach, R. Feldman, J. C. Saccavini, G. Tobias, B. Ballesteros, K. T. Al-Jamal and T. Da Ros, *J. Mater. Chem. B*, 2021, **10**, 47–56.
38 Y. Yin, Y. Li, S. Wang, Z. Dong, C. Liang, J. Sun, C. Wang, R. Chai, W. Fei, J. Zhang, M. Qi, L. Feng and Q. Zhang, *J. Nanobiotechnol.*, 2021, **19**, 80.
39 Y. Kanehira, K. Togami, K. Ishizawa, S. Sato, H. Tada and S. Chono, *Pharm. Dev. Technol.*, 2019, **24**, 1095–1103.
40 P. Patel, M. Raval, A. Manvar, V. Airao, V. Bhatt and P. Shah, *PLoS One*, 2022, **17**, e0267257.
41 S. H. Jeong, J. H. Jang and Y. B. Lee, *J. Controlled Release*, 2021, **335**, 86–102.
42 N. N. Parayath, A. Parikh and M. M. Amiji, *Nano Lett.*, 2018, **18**, 3571–3579.
43 S. V. Vinogradov, T. K. Bronich and A. V. Kabanov, *Adv. Drug Delivery Rev.*, 2002, **54**, 135–147.
44 E. Pérez-Herrero and A. Fernández-Medarde, *Eur. J. Pharm. Biopharm.*, 2015, **93**, 52–79.

45 L. Zhang, G. Xie, X. Xiao and C. Cheng, *J. Cancer Res. Clin. Oncol.*, 2022, DOI: 10.1007/s00432-022-04298-2.
46 W. Yao, J. Yao, F. Qian, Z. Que, P. Yu, T. Luo, D. Zheng, Z. Zhang and J. Tian, *Acta Biochim. Biophys. Sin.*, 2021, **53**, 1027–1036.
47 K. Mao, W. Zhang, L. Yu, Y. Yu, H. Liu and X. Zhang, *Drug Des., Dev. Ther.*, 2021, **15**, 3475–3486.
48 N. Zhu, G. Li, J. Zhou, Y. Zhang, K. Kang, B. Ying, Q. Yi and Y. Wu, *J. Mater. Chem. B*, 2021, **9**, 2483–2493.
49 O. Knights, S. Freear and J. R. McLaughlan, *Nanomaterials*, 2020, **10**, 1307.
50 S. Fu, Y. Zhao, J. Sun, T. Yang, D. Zhi, E. Zhang, F. Zhong, Y. Zhen, S. Zhang and S. Zhang, *Colloids Surf., B*, 2021, **201**, 111623.
51 L. Ren, Y. J. Kim, S. Y. Park, S. Lee, J. Y. Lee, C. P. Park and Y. T. Lim, *J. Mater. Chem. B*, 2016, **4**, 4832–4838.
52 B. Wang, W. Hu, H. Yan, G. Chen, Y. Zhang, J. Mao and L. Wang, *Biomed. Pharmacother.*, 2021, **136**, 111249.
53 K. Thangavel, A. Lakshmikuttyamma, C. Thangavel and S. A. Shoyele, *Colloids Surf., B*, 2022, **209**, 112162.
54 P. D. Ganthala, S. Alavala, N. Chella, S. B. Andugulapati, N. B. Bathini and R. Sistla, *Colloids Surf., B*, 2022, **211**, 112305.
55 S. González-Rubio, C. Salgado, V. Manzaneda-González, M. Muñoz-Úbeda, R. Ahijado-Guzmán, P. Natale, V. G. Almendro-Vedia, E. Junquera, J. O. Barcina, I. Ferrer, A. Guerrero-Martínez, L. Paz-Ares and I. López-Montero, *Nanoscale*, 2022, **14**, 8028–8040.
56 Z. Ma, S. W. Wong, H. Forgham, L. Esser, M. Lai, M. N. Leiske, K. Kempe, G. Sharbeen, J. Youkhana, F. Mansfeld, J. F. Quinn, P. A. Phillips, T. P. Davis, M. Kavallaris and J. A. McCarroll, *Biomaterials*, 2022, **285**, 121539.
57 V. Patel, R. Lalani, I. Vhora, D. Bardoliwala, A. Patel, S. Ghosh and A. Misra, *Drug Delivery Transl. Res.*, 2021, **11**, 2052–2071.
58 S. Wang, Y. Chen, J. Guo and Q. Huang, *Int. J. Mol. Sci.*, 2023, **24**, 2643.
59 H. Abbasi, N. Rahbar, M. Kouchak, P. Khalil Dezfuli and S. Handali, *J. Liposome Res.*, 2022, **32**, 195–210.
60 M. Dymek and E. Sikora, *Adv. Colloid Interface Sci.*, 2022, **309**, 102757.
61 H. S. Oberoi, N. V. Nukolova, A. V. Kabanov and T. K. Bronich, *Adv. Drug Delivery Rev.*, 2013, **65**, 1667–1685.
62 A. Akbarzadeh, R. Rezaei-Sadabady, S. Davaran, S. W. Joo, N. Zarghami, Y. Hanifehpour, M. Samiei, M. Kouhi and K. Nejati-Koshki, *Nanoscale Res. Lett.*, 2013, **8**, 102.
63 W. Men, P. Zhu, S. Dong, W. Liu, K. Zhou, Y. Bai, X. Liu, S. Gong and S. Zhang, *Drug Delivery*, 2020, **27**, 180–190.
64 J. German-Cortés, M. Vilar-Hernández, D. Rafael, I. Abasolo and F. Andrade, *Pharmaceutics*, 2023, **15**, 831.
65 S. V. Khairnar, P. Pagare, A. Thakre, A. R. Nambiar, V. Junnuthula, M. C. Abraham, P. Kolimi, D. Nyavanandi and S. Dyawanapelly, *Pharmaceutics*, 2022, **14**, 1886.
66 V. Gugleva and V. Andonova, *Pharmaceuticals*, 2023, **16**, 474.
67 E. Salah, M. M. Abouelfetouh, Y. Pan, D. Chen and S. Xie, *Colloids Surf., B*, 2020, **196**, 111305.
68 A. R. SA, A. Mohd Gazzali, F. A. Fisol, M. A. Ibrahim, T. Parumasivam, N. Mohtar and A. W. Habibah, *Cancers*, 2021, **13**, 400.
69 V. Mishra, K. K. Bansal, A. Verma, N. Yadav, S. Thakur, K. Sudhakar and J. M. Rosenholm, *Pharmaceutics*, 2018, **10**, 191.
70 M. Najlah, Z. Ahmed, M. Iqbal, Z. Wang, P. Tawari, W. Wang and C. McConville, *Eur. J. Pharm. Biopharm.*, 2017, **112**, 224–233.
71 M. Haim Zada, Y. Rottenberg and A. J. Domb, *J. Colloid Interface Sci.*, 2022, **622**, 904–913.
72 S. R. Schaffazick, A. R. Pohlmann, T. Dalla-Costa and S. S. Guterres, *Eur. J. Pharm. Biopharm.*, 2003, **56**, 501–505.
73 N. A. N. Hanafy, M. El-Kemary and S. Leporatti, *Cancers*, 2018, **10**, 238.
74 M. Zhang, Z. Zhang, X. Song, J. Zhu, J. A. Sng, J. Li and Y. Wen, *Biomacromolecules*, 2022, **23**, 4586–4596.
75 S. Perumal, R. Atchudan and W. Lee, *Polymers*, 2022, **14**, 2510.
76 C. Oerlemans, W. Bult, M. Bos, G. Storm, J. F. Nijsen and W. E. Hennink, *Pharm. Res.*, 2010, **27**, 2569–2589.
77 A. P. Sherje, M. Jadhav, B. R. Dravyakar and D. Kadam, *Int. J. Pharm.*, 2018, **548**, 707–720.
78 A. D. Dey, A. Bigham, Y. Esmaeili, M. Ashrafizadeh, F. D. Moghaddam, S. C. Tan, S. Yousefiasl, S. Sharma, A. Maleki, N. Rabiee, A. P. Kumar, V. K. Thakur, G. Orive, E. Sharifi, A. Kumar and P. Makvandi, *Semin. Cancer Biol.*, 2022, **86**, 396–419.
79 X. Li, A. Naeem, S. Xiao, L. Hu, J. Zhang and Q. Zheng, *Pharmaceutics*, 2022, **14**, 1292.
80 C. Sandoval-Yañez and C. Castro Rodriguez, *Materials*, 2020, **13**, 570.
81 A. S. Chauhan, *Molecules*, 2018, **23**, 938.
82 H. Y. Lee, K. A. Mohammed and N. Nasreen, *Am. J. Cancer Res.*, 2016, **6**, 1118–1134.
83 M. Sun, T. Wang, L. Li, X. Li, Y. Zhai, J. Zhang and W. Li, *Front. Pharmacol.*, 2021, **12**, 702445.
84 Y. Liu, W. Ma and J. Wang, *Curr. Pharm. Des.*, 2018, **24**, 2719–2728.
85 P. Singh, S. Pandit, V. Mokkapati, A. Garg, V. Ravikumar and I. Mijakovic, *Int. J. Mol. Sci.*, 2018, **19**, 1979.
86 A. Bardestani, S. Ebrahimpour, A. Esmaeili and A. Esmaeili, *J. Nanobiotechnol.*, 2021, **19**, 327.
87 V. Frantellizzi, M. Conte, M. Pontico, A. Pani, R. Pani and G. De Vincentis, *Nucl. Med. Mol. Imaging*, 2020, **54**, 65–80.
88 Z. Wang, R. Qiao, N. Tang, Z. Lu, H. Wang, Z. Zhang, X. Xue, Z. Huang, S. Zhang, G. Zhang and Y. Li, *Biomaterials*, 2017, **127**, 25–35.
89 L. M. Ngema, S. A. Adeyemi, T. Marimuthu and Y. E. Choonara, *Int. J. Pharm.*, 2021, **606**, 120870.
90 M. Nejabat, F. Charbgoo and M. Ramezani, *J. Biomed. Mater. Res.*, 2017, **105**, 2355–2367.
91 V. Mishra, A. Patil, S. Thakur and P. Kesharwani, *Drug Discovery Today*, 2018, **23**, 1219–1232.
92 C. Woodman, G. Vundu, A. George and C. M. Wilson, *Semin. Cancer Biol.*, 2021, **69**, 349–364.

93 J. Ackermann, J. T. Metternich, S. Herbertz and S. Kruss, *Angew. Chem., Int. Ed. Engl.*, 2022, **61**, e202112372.
94 Z. Pu, Y. Wei, Y. Sun, Y. Wang and S. Zhu, *Int. J. Nanomed.*, 2022, **17**, 6157–6180.
95 D. Cai, D. Blair, F. J. Dufort, M. R. Gumina, Z. Huang, G. Hong, D. Wagner, D. Canahan, K. Kempa, Z. F. Ren and T. C. Chiles, *Nanotechnology*, 2008, **19**, 1–10.
96 A. M. Elhissi, W. Ahmed, I. U. Hassan, V. R. Dhanak and A. D'Emanuele, *J. Drug Delivery*, 2012, **2012**, 837327.
97 J. Y. Oh, G. Yang, E. Choi and J. H. Ryu, *Biomater. Sci.*, 2022, **10**, 1448–1455.
98 Y. Feng, Z. Liao, M. Li, H. Zhang, T. Li, X. Qin, S. Li, C. Wu, F. You, X. Liao, L. Cai, H. Yang and Y. Liu, *Adv. Healthcare Mater.*, 2022, e2201884, DOI: **10.1002/adhm.202201884**.
99 S. Shah, P. Famta, D. Bagasariya, K. Charankumar, A. Sikder, R. Kashikar, A. K. Kotha, M. B. Chougule, D. K. Khatri, A. Asthana, R. S. Raghuvanshi, S. B. Singh and S. Srivastava, *Mol. Pharm.*, 2022, **19**, 4428–4452.
100 P. Yang, S. Gai and J. Lin, *Chem. Soc. Rev.*, 2012, **41**, 3679–3698.
101 I. I. Slowing, J. L. Vivero-Escoto, C. W. Wu and V. S. Lin, *Adv. Drug Delivery Rev.*, 2008, **60**, 1278–1288.
102 C. T. Badea, K. K. Athreya, G. Espinosa, D. Clark, A. P. Ghafoori, Y. Li, D. G. Kirsch, G. A. Johnson, A. Annapragada and K. B. Ghaghada, *PLoS One*, 2012, **7**, e34496.
103 S. M. Jo, Y. Kim, Y. S. Jeong, Y. Hee Oh, K. Park and H. S. Kim, *Biosens. Bioelectron.*, 2013, **46**, 142–149.
104 D. A. Tomalia, L. A. Reyna and S. Svenson, *Biochem. Soc. Trans.*, 2007, **35**, 61–67.
105 H. Kobayashi, C. Wu, M. K. Kim, C. H. Paik, J. A. Carrasquillo and M. W. Brechbiel, *Bioconjugate Chem.*, 1999, **10**, 103–111.
106 E. C. Wiener, M. W. Brechbiel, H. Brothers, R. L. Magin, O. A. Gansow, D. A. Tomalia and P. C. Lauterbur, *Magn. Reson. Med.*, 1994, **31**, 1–8.
107 H. Z. Zhu, J. Hou, Y. Guo, X. Liu, F. L. Jiang, G. P. Chen, X. F. Pang, J. G. Sun and Z. T. Chen, *Drug Delivery*, 2018, **25**, 1974–1983.
108 P. Iranpour, M. Ajamian, A. Safavi, N. Iranpoor, A. Abbaspour and S. Javanmardi, *J. Mater. Sci.: Mater. Med.*, 2018, **29**, 48.
109 J. F. Hainfeld, D. N. Slatkin, T. M. Focella and H. M. Smilowitz, *Br. J. Radiol.*, 2006, **79**, 248–253.
110 H. S. Zhou, I. I. Honma, H. Komiyama and J. W. Haus, *Phys. Rev. B: Condens. Matter Mater. Phys.*, 1994, **50**, 12052–12056.
111 O. Barash, N. Peled, U. Tisch, P. A. Bunn, Jr., F. R. Hirsch and H. Haick, *Nanomed*, 2012, **8**, 580–589.
112 K. Hu, J. Cheng, K. Wang, Y. Zhao, Y. Liu, H. Yang and Z. Zhang, *Talanta*, 2022, **238**, 122987.
113 S. Benderbous, C. Corot, P. Jacobs and B. Bonnemain, *Acad. Radiol.*, 1996, **3**(Suppl 2), S292–S294.
114 S. Park, B. B. Cho, J. R. Anusha, S. Jung, C. Justin Raj, B. C. Kim and K. H. Yu, *J. Nanosci. Nanotechnol.*, 2020, **20**, 2040–2044.
115 M. Longmire, P. L. Choyke and H. Kobayashi, *Nanomedicine*, 2008, **3**, 703–717.
116 Z. Zhao, M. Zhen, C. Zhou, L. Li, W. Jia, S. Liu, X. Li, X. Liao and C. Wang, *J. Mater. Chem. B*, 2021, **9**, 5722–5728.
117 J. Grebowski and G. Litwinienko, *Eur. J. Med. Chem.*, 2022, **238**, 114481.
118 N. B. Fernandes, R. U. K. Shenoy, M. K. Kajampady, D. C. CEM, R. K. Shirodkar, L. Kumar and R. Verma, *Environ. Sci. Pollut. Res. Int.*, 2022, **29**, 58607–58627.
119 R. D. Bolskar, A. F. Benedetto, L. O. Husebo, R. E. Price, E. F. Jackson, S. Wallace, L. J. Wilson and J. M. Alford, *J. Am. Chem. Soc.*, 2003, **125**, 5471–5478.
120 A. Aasi, S. M. Aghaei and B. Panchapakesan, *Nanotechnology*, 2020, **31**, 415707.
121 J. L. Vivero-Escoto, K. M. Taylor-Pashow, R. C. Huxford, J. Della Rocca, C. Okoruwa, H. An, W. Lin and W. Lin, *Small*, 2011, **7**, 3519–3528.
122 M. S. Kang, R. K. Singh, T. H. Kim, J. H. Kim, K. D. Patel and H. W. Kim, *Acta Biomater.*, 2017, **55**, 466–480.
123 C. Gai, C. Liu, X. Wu, M. Yu, J. Zheng, W. Zhang, S. Lv and W. Li, *Cell Death Dis.*, 2020, **11**, 751.
124 R. Kedmi, N. Ben-Arie and D. Peer, *Biomaterials*, 2010, **31**, 6867–6875.
125 C. Butts, M. A. Socinski, P. L. Mitchell, N. Thatcher, L. Havel, M. Krzakowski, S. Nawrocki, T. E. Ciuleanu, L. Bosquée, J. M. Trigo, A. Spira, L. Tremblay, J. Nyman, R. Ramlau, G. Wickart-Johansson, P. Ellis, O. Gladkov, J. R. Pereira, W. E. Eberhardt, C. Helwig, A. Schröder and F. A. Shepherd, *Lancet Oncol.*, 2014, **15**, 59–68.
126 A. Ravaioli, M. Papi, E. Pasquini, M. Marangolo, B. Rudnas, M. Fantini, S. V. Nicoletti, F. Drudi, I. Panzini, E. Tamburini, L. Gianni and G. Pasini, *J. Chemother.*, 2009, **21**, 86–90.
127 A. A. Tarhini, C. P. Belani, J. D. Luketich, A. Argiris, S. S. Ramalingam, W. Gooding, A. Pennathur, D. Petro, K. Kane, D. Liggitt, T. Championsmith, X. Zhang, M. W. Epperly and J. S. Greenberger, *Hum. Gene Ther.*, 2011, **22**, 336–342.
128 L. Kelland, *Expert Opin. Invest. Drugs*, 2007, **16**, 1009–1021.
129 S. C. White, P. Lorigan, G. P. Margison, J. M. Margison, F. Martin, N. Thatcher, H. Anderson and M. Ranson, *Br. J. Cancer*, 2006, **95**, 822–828.
130 K. H. Bae, J. Y. Lee, S. H. Lee, T. G. Park and Y. S. Nam, *Adv. Healthcare Mater.*, 2013, **2**, 576–584.
131 Y. Yang, Z. Huang, J. Li, Z. Mo, Y. Huang, C. Ma, W. Wang, X. Pan and C. Wu, *Adv. Healthcare Mater.*, 2019, **8**, e1900965.
132 C. Tapeinos, M. Battaglini and G. Ciofani, *J. Controlled Release*, 2017, **264**, 306–332.
133 J. Huang, C. Zhuang, J. Chen, X. Chen, X. Li, T. Zhang, B. Wang, Q. Feng, X. Zheng, M. Gong, Q. Gong, K. Xiao, K. Luo and W. Li, *Adv. Mater.*, 2022, **34**, e2201516.
134 F. Gong, R. Wang, Z. Zhu, J. Duan, X. Teng and Z. K. Cui, *Drug Delivery*, 2020, **27**, 238–247.
135 Z. Wang, J. Wen, H. Liu, L. Zheng, H. Luo, Z. Liu, X. Chen, F. Wang, D. Li, H. Pei, W. Li and L. Chen, *J. Biomed. Nanotechnol.*, 2018, **14**, 1225–1238.
136 F. Zhu, L. Xu, X. Li, Z. Li, J. Wang, H. Chen, X. Li and Y. Gao, *Eur. J. Pharm. Sci.*, 2021, **167**, 106004.

137 N. Maghsoudnia, R. B. Eftekhari, A. N. Sohi and F. A. Dorkoosh, *Curr. Drug Delivery*, 2021, **18**, 31–43.
138 G. J. Weiss, J. Chao, J. D. Neidhart, R. K. Ramanathan, D. Bassett, J. A. Neidhart, C. H. J. Choi, W. Chow, V. Chung, S. J. Forman, E. Garmey, J. Hwang, D. L. Kalinoski, M. Koczywas, J. Longmate, R. J. Melton, R. Morgan, J. Oliver, J. J. Peterkin, J. L. Ryan, T. Schluep, T. W. Synold, P. Twardowski, M. E. Davis and Y. Yen, *Invest. New Drugs*, 2013, **31**, 986–1000.
139 H. K. Ahn, M. Jung, S. J. Sym, D. B. Shin, S. M. Kang, S. Y. Kyung, J. W. Park, S. H. Jeong and E. K. Cho, *Cancer Chemother. Pharmacol.*, 2014, **74**, 277–282.
140 S. R. Volovat, T. E. Ciuleanu, P. Koralewski, J. E. G. Olson, A. Croitoru, K. Koynov, S. Stabile, G. Cerea, A. Osada, I. Bobe and C. Volovat, *Oncotarget*, 2020, **11**, 3105–3117.
141 S. P. Chawla, S. Goel, W. Chow, F. Braiteh, A. S. Singh, J. E. G. Olson, A. Osada, I. Bobe and R. F. Riedel, *Clin. Cancer Res.*, 2020, **26**, 4225–4232.
142 D. D. Von Hoff, M. M. Mita, R. K. Ramanathan, G. J. Weiss, A. C. Mita, P. M. LoRusso, H. A. Burris, 3rd, L. L. Hart, S. C. Low, D. M. Parsons, S. E. Zale, J. M. Summa, H. Youssoufian and J. C. Sachdev, *Clin. Cancer Res.*, 2016, **22**, 3157–3163.
143 J. Peng, R. Wang, W. Sun, M. Huang, R. Wang, Y. Li, P. Wang, G. Sun and S. Xie, *Biomater. Sci.*, 2021, **9**, 6528–6541.
144 J. Ma, C. Wen, M. Chen, W. Zhang, L. Wang and H. Yin, *ACS Biomater. Sci. Eng.*, 2023, **9**, 2793–2805.
145 L. M. Ngema, S. A. Adeyemi, T. Marimuthu, P. Ubanako, D. Wamwangi and Y. E. Choonara, *Pharmaceutics*, 2022, **14**, 829.
146 Q. Qin, Y. Zhou, P. Li, Y. Liu, R. Deng, R. Tang, N. Wu, L. Wan, M. Ye, H. Zhou and Z. Wang, *J. Nanobiotechnol.*, 2023, **21**, 131.
147 S. Augustine, B. Prabhakar and P. Shende, *Curr. Drug Delivery*, 2022, **19**, 697–705.
148 M. Ahamed, M. J. Akhtar and H. A. Alhadlaq, *Environ. Sci. Pollut. Res. Int.*, 2022, **29**, 87844–87857.
149 J. Lin, R. Zheng, L. Huang, Y. Tu, X. Li and J. Chen, *Colloids Surf., B*, 2022, **217**, 112639.
150 H. Wu, W. H. Lv, Y. Y. Zhu, Y. Y. Jia and F. Nie, *Eur. J. Pharm. Sci.*, 2023, **182**, 106372.
151 N. R. Mehta, G. T. Wurz, R. A. Burich, B. E. Greenberg, S. Griffey, A. Gutierrez, K. E. Bell, J. L. McCall, M. Wolf and M. DeGregorio, *Clin. Cancer Res.*, 2012, **18**, 2861–2871.
152 N. N. Parayath, S. K. Gandham and M. M. Amiji, *Nanomedicine*, 2022, **17**, 1355–1373.
153 E. J. Shillitoe, *Head Neck Oncol.*, 2009, **1**, 7.
154 N. Yanaihara, N. Caplen, E. Bowman, M. Seike, K. Kumamoto, M. Yi, R. M. Stephens, A. Okamoto, J. Yokota, T. Tanaka, G. A. Calin, C. G. Liu, C. M. Croce and C. C. Harris, *Cancer Cell*, 2006, **9**, 189–198.
155 A. L. Kasinski and F. J. Slack, *Cancer Res.*, 2012, **72**, 5576–5587.
156 M. S. Kumar, S. J. Erkeland, R. E. Pester, C. Y. Chen, M. S. Ebert, P. A. Sharp and T. Jacks, *Proc. Natl. Acad. Sci. U. S. A.*, 2008, **105**, 3903–3908.
157 J. F. Wiggins, L. Ruffino, K. Kelnar, M. Omotola, L. Patrawala, D. Brown and A. G. Bader, *Cancer Res.*, 2010, **70**, 5923–5930.
158 Z. Bai, J. Wei, C. Yu, X. Han, X. Qin, C. Zhang, W. Liao, L. Li and W. Huang, *J. Mater. Chem. B*, 2019, **7**, 1209–1225.
159 J. McCarroll, J. Teo, C. Boyer, D. Goldstein, M. Kavallaris and P. A. Phillips, *Front. Physiol.*, 2014, **5**, 2.
160 J. A. McCarroll, T. Dwarte, H. Baigude, J. Dang, L. Yang, R. B. Erlich, K. Kimpton, J. Teo, S. M. Sagnella, M. C. Akerfeldt, J. Liu, P. A. Phillips, T. M. Rana and M. Kavallaris, *Oncotarget*, 2015, **6**, 12020–12034.
161 X. Zhu, Y. Xu, L. M. Solis, W. Tao, L. Wang, C. Behrens, X. Xu, L. Zhao, D. Liu, J. Wu, N. Zhang, I. I. Wistuba, O. C. Farokhzad, B. R. Zetter and J. Shi, *Proc. Natl. Acad. Sci. U. S. A.*, 2015, **112**, 7779–7784.
162 A. M. Davies, D. R. Gandara, P. N. Lara, Jr., P. C. Mack, D. H. Lau and P. H. Gumerlock, *Clin. Lung Cancer*, 2003, **4**(Suppl 2), S68–S73.
163 S. Chaudhary, A. Singh, P. Kumar and M. Kaushik, *J. Biochem. Mol. Toxicol.*, 2021, **35**, e22784.
164 N. Amreddy, A. Babu, R. Muralidharan, A. Munshi and R. Ramesh, *Top. Curr. Chem.*, 2017, **375**, 35.
165 M. Talekar, M. Trivedi, P. Shah, Q. Ouyang, A. Oka, S. Gandham and M. M. Amiji, *Mol. Ther.*, 2016, **24**, 759–769.
166 I. Ito, L. Ji, F. Tanaka, Y. Saito, B. Gopalan, C. D. Branch, K. Xu, E. N. Atkinson, B. N. Bekele, L. C. Stephens, J. D. Minna, J. A. Roth and R. Ramesh, *Cancer Gene Ther.*, 2004, **11**, 733–739.
167 E. Huynh and G. Zheng, *Wiley Interdiscip. Rev.: Nanomed. Nanobiotechnol.*, 2013, **5**, 250–265.
168 X. H. Do, T. D. Nguyen, T. T. H. Le, T. T. To, T. V. K. Bui, N. H. Pham, K. Lam, T. M. N. Hoang and P. T. Ha, *Pharmaceutics*, 2023, **15**, 1523.
169 S. Wang, Q. You, J. Wang, Y. Song, Y. Cheng, Y. Wang, S. Yang, L. Yang, P. Li, Q. Lu, M. Yu and N. Li, *Nanoscale*, 2019, **11**, 6270–6284.
170 Q. Xiao, Y. Lu, M. Chen, B. Chen, Y. Yang, D. Cui, B. Pan and N. Xu, *Nanoscale Res. Lett.*, 2018, **13**, 77.